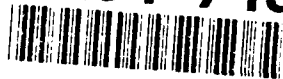


AD-A261 713



AD-A261 713

DTIC
ELECTE
MAR 5 1993
S C D

AIR FORCE OFFICE OF SCIENTIFIC RESEARCH

FINAL REPORT

for period November 1, 1988 to September 30, 1992

GRANT NO. F46920-89-C-004⁰⁰⁰⁴

entitled

OPTICAL CHARACTERIZATION OF

$\text{Ga}_{1-x}\text{In}_x\text{As}_y\text{Sb}_{1-y}/\text{GaSb}$

ALLOY AND DEVICE APPLICATION

by

Shanthi N. Iyer and Ali Abul Fadl
Department of Electrical Engineering
North Carolina A & T State University
Greensboro, NC 27411

93-04653



93-04653

Standard Form 298 (Rev. 2-89)
Prescribed by ANSI Std. Z39.18
298-102

TABLE OF CONTENTS

	PAGE
TITLE PAGE	
ABSTRACT	i
REPORT	
I. INTRODUCTION	1
II. LPEE GROWTH	2
III. OPTICAL CHARACTERIZATION	
A. Low temperature PL studies of GaSb and GaInAsSb	5
B. Low temperature PL studies of Te-Doped GaSb	7
C. Photoreflectance	12
IV. GaSb PHOTODIODE	16
V. BIBLIOGRAPHY	20
VI. PUBLICATIONS AND THESIS ARISING FROM AFOSR	22

APPENDIX

- A. LPEE Growth of GaSb and GaInAsSb (MRS Symp. Proc.)
- B. Growth and PL of GaSb & $\text{Ga}_{1-x}\text{In}_x\text{As}_y\text{Sb}_{1-y}$ Grown on GaSb
 Substrates by LPEE (Phys. Rev. B)
- C. PL Study of LPEE Grown GaInAsSb on (100) GaSb (J. Appl. Phys.)

Accession For	
NTIS CRA&I	<input checked="" type="checkbox"/>
DTIC TAB	<input type="checkbox"/>
Unannounced	<input type="checkbox"/>
Justification	
By	
Distribution /	
Availability Codes	
Dist	Avail and/or Special
A-1	

ABSTRACT

During the period of this research grant, GaSb and GaInAsSb layers of excellent optical quality with compositions corresponding to the room temperature photoluminescence peak wavelength of $1.7\text{ }\mu\text{m}$ to $2.32\text{ }\mu\text{m}$ have been grown by liquid phase electroepitaxial ((LPEE) technique. These layers were characterized using X-ray diffraction, energy dispersive X-ray analysis and low temperature Fourier transform photoluminescence (PL) with emphasis on the latter.

The variation in the low temperature photoluminescence spectra of these alloys as a function of the alloy compositions has been the subject of detailed investigation. The nature of the recombination processes has been identified from the temperature and intensity dependence of the PL spectra. A systematic trend in the low temperature PL spectra is observed with the change in the alloy composition. GaSb and GaInAsSb with compositions close to GaSb exhibit several bound exciton peaks which have been attributed to different neutral acceptors.

N-type doping of the layers has been achieved using tellurium. The PL spectra become increasingly complicated and transitions associated with deeper acceptor levels and the second ionization level of the shallow native residual acceptor at 34 meV above the valence band, which are either weak or absent in undoped GaSb, become dominant. Considerable change in the PL spectra with the excitation intensity is also observed. A systematic and quantitative evaluation of the effects of compensation in GaSb has been examined as a function of Te concentration in the layers under both low and high excitation conditions.

Another optical characterization technique, photoreflectance spectroscopy has been assembled for the characterization of semiconductor band structure and surface, however no PR signals were detected on GaSb layers and will be the focus of future research efforts. PIN photodiode device has been fabricated using the doped layers and characterized using I-V and C-V measurements.

Grant# F46920-89-C-004, funded for \$292,095 from 11/1/88-9/30/92
Project Title: OPTICAL CHARACTERIZATION OF $\text{Ga}_{1-x}\text{In}_x\text{As}_y\text{Sb}_{1-y}$ /GaSb ALLOY
AND DEVICE APPLICATION

This is a final technical report describing the research activities of the above AFOSR grant. The three year grant period began on Nov 1, 1988 and was extended on a no-cost basis for a year up to Sept. 30, 1992. This program involved the effort of two faculty members, four MSEE students and one undergraduate student. During this period, there has also been collaborative efforts with other institutions. Dr. Al Macrander and Mr. Soon Lau from AT&T Bell Labs at Murray Hill, NJ very generously carried out the X-ray diffraction measurements for lattice mismatch on number of GaInAsSb samples grown in the initial phase of the grant period. AFOSR also promoted close collaboration with Dr. Mitchel's group at Wright Laboratories, WPAFB. Collaboration was also established during this period with Dr. K.K. Bajaj a well known theoretician from Emory university. These collaborations were extremely fruitful and permitted rapid advances outlined in this report. During this entire grant period, the suggestions from technical monitor Dr. Gernot Pomrenke were extremely helpful.

The tasks proposed in the original proposal were modified throughout the grant period depending on the progress made in various focussed areas of interest, availability and accessibility of the equipments. The major thrusts in the research work during this period could be broadly classified into three categories:

1. LPEE growth: LPEE growth of GaSb and GaInAsSb alloy system.
2. Optical Characterization:
 - (a) Low temperature photoluminescence studies of undoped GaSb and GaInAsSb alloys.
 - (b) Low temperature photoluminescence studies of Te doped GaSb and GaInAsSb alloys.
 - (c) Photoreflectance.
3. PIN photodiode.

The following sections review the various technical accomplishments. A few of the above work has either already been published or under print and hence will not be elaborated in the text of the report and the reprint/original manuscript of the paper submitted to the journals are attached in the Appendix of this report.

I INTRODUCTION

The quaternary alloys $\text{Ga}_x\text{In}_{1-x}\text{As}_y\text{Sb}_{1-y}$ are currently of great interest for use in infrared devices. This alloy system lattice matched to GaInAsSb (1.71 - 4.2 μm) covers the range where the fluoride based fibers are predicted to exhibit low loss and dispersion, in the 2-4 μm wavelength range. Hence, they have potential application for future fiber communication system. Furthermore, the theoretically predicted high carrier mobility in GaSb makes it an attractive candidate for microwave devices.

GaInAsSb quaternary alloys have usually been grown by liquid phase epitaxy with only a few reports in the literature of growth by molecular beam epitaxy (MBE) (1,2) and metal-organic chemical vapor deposition (MOCVD) (3,4). A notable feature of this alloy system is

the presence of a large miscibility gap covering almost the entire composition range at typical growth temperatures. Hence, the compositions grown by the near equilibrium techniques, e.g. LPE and LPEE is limited to a very narrow range 1.7-2.32 μ m towards the GaSb corner of the phase diagram (5-13). However, other techniques, namely, MBE and MOCVD have been successful in penetrating the miscibility gap due to their nonequilibrium nature of the growth process. The extent to which this miscibility gap is penetrated depends on the particular technique. Molecular beam epitaxy(MBE) has been successful in penetrating the miscibility gap only a little. The longest wavelength so far reported on this system by this technique is 2.5 μ m(1). Organometallic vapor phase epitaxy (MOVPE) (3,4,14) technique has been successfully used for the growth of these layers throughout the miscibility gap, however evidence of compositional clustering has been reported (3) for layers in the miscibility gap. The extent to which this affects the performance of GaInAsSb based optical devices is presently unknown.

However LPE and LPEE are still attractive growth techniques as they are inexpensive and particularly for compounds where there exists problems with other growth techniques either due to the toxicity of the gases used or the reproducibility.

In LPEE technique, the growth is induced and sustained by an external parameter, namely, the current density, and is carried out at a constant furnace temperature. Hence the interface stability(15), surface morphology(16) and the compositional uniformity(17,18) of the layers grown by this technique have shown to be considerably improved over those by conventional LPE technique. *With the financial support from AFOSR, LPEE technique has been used to grow GaSb and GaInAsSb layers for the first time.*

II LPEE GROWTH

The first phase of the work involved the determination of the necessary growth conditions for the growth of GaSb and GaInAsSb epilayers on (100) GaSb by liquid phase electroepitaxial (LPEE) technique, and to determine the extent to which the miscibility gap can be penetrated by this technique.

The multiple well horizontal slider boat system was built. The body of the boat consists of two high purity graphite which are insulated from each other by quartz spacers, and a graphite slider as shown in Fig.1 . The latter consists of a dummy well containing the GaSb melt for the back contact, a boron nitride substrate recess to hold the substrate and two rectangular strips of boron-nitride. The purpose of boron nitride is to insulate the slider from the top part of the graphite thus ensuring that the current passes only through the melt-substrate interface, when the substrate is slid underneath the melt. A quartz rod which is interlocked with the graphite plunger serves as a push rod to drive the melt back and forth, in order to make and break the electrical contact, respectively with the substrate. The boat has been designed for multilayer growth on the substrate of small size (6mm x 6mm). The temperature profile on the boat was typically 1°C over 6 cm length of the boat. We have grown layers of GaSb and GaInAsSb in the composition range corresponding to a wavelength range of 1.689 μ m to 2.32 μ m.

The liquidus data for different compositions of grown layers are detailed in Ref.11. Figure 2 shows our results on the variation of the distribution coefficient k , of the different

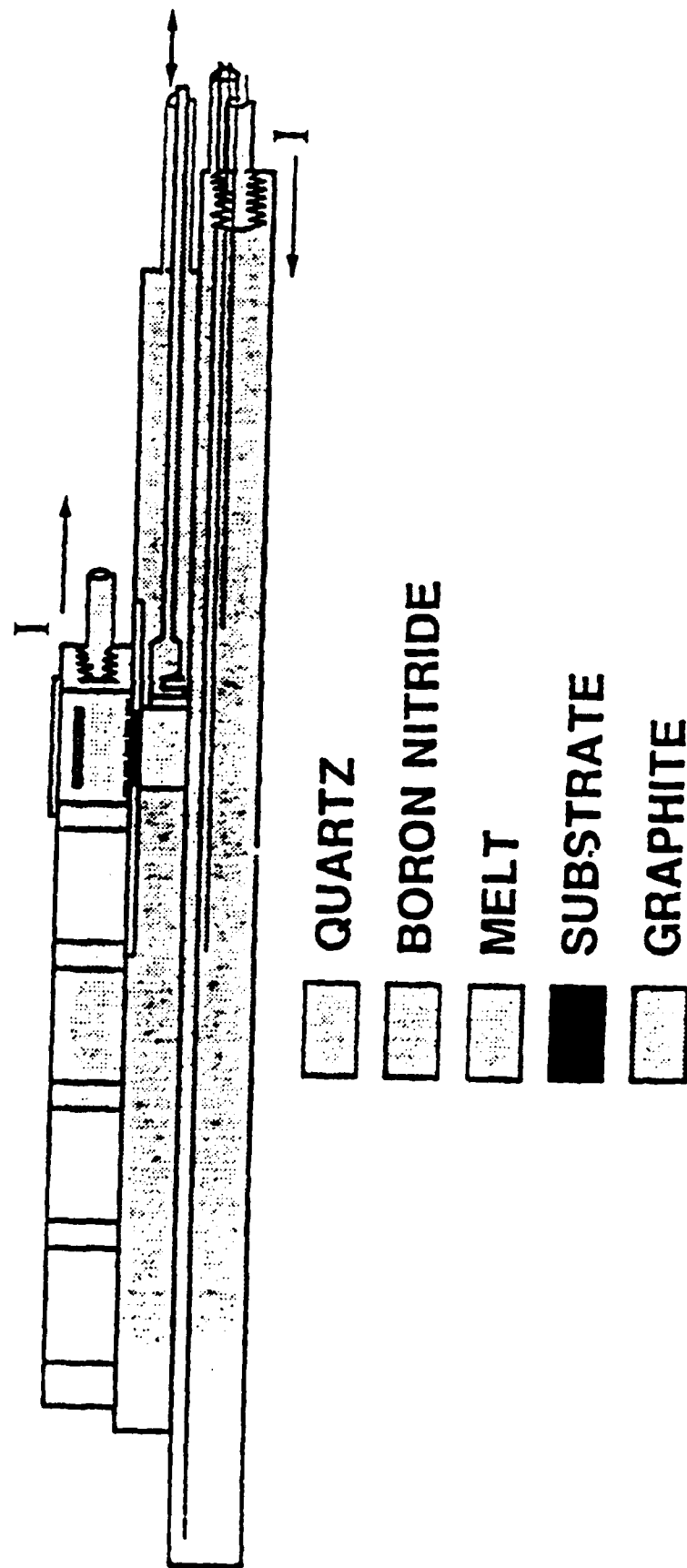


Figure 1. Schematic diagram of the LPEE growth set-up.

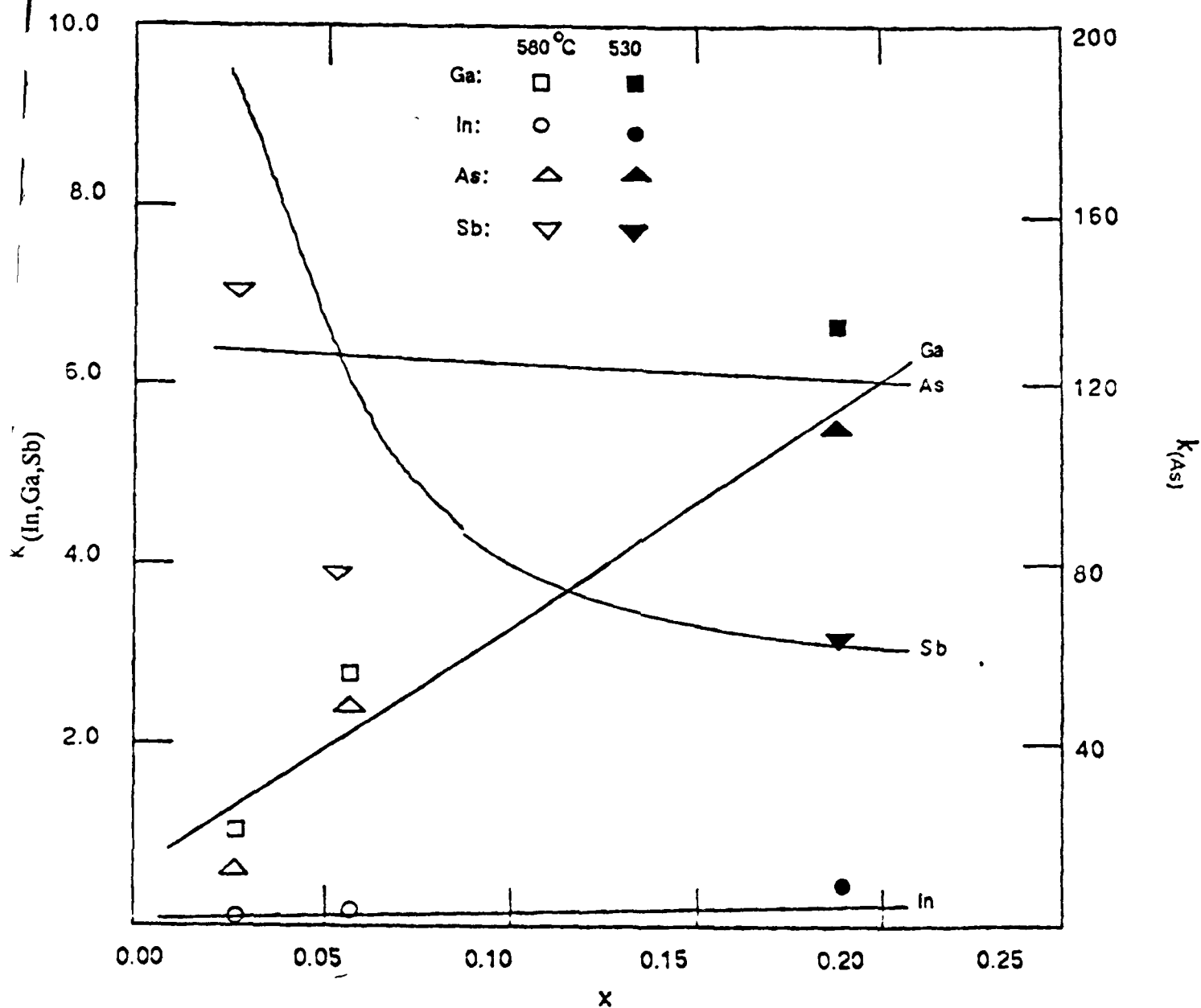


Figure 2. Variation of the distribution coefficient of the different elements as a function of solid composition x . The data include our work represented by open and closed points at 580° C and 530° C, respectively. The solid line represents the data from Ref.5.

elements with the solidus composition of the alloy along with the values reported by DeWinter et al.(5) at around 530°C. Though the data is limited, it may be noted that the distribution coefficient of As is one order of magnitude higher than the other elements. With change in temperature the major variation occurs in the distribution coefficient of As, k_{As} , which showed a large decrease with increase in growth temperature and hence it is expected that the layers grown at temperatures higher than 580°C would exhibit better compositional homogeneity. Hence layers were grown at 580°C. However, for compositions towards InAs, due to the melt instability growth temperature had to be lowered to 530°C(see for details Ref. 11, Appendix A).

The surface morphology is found to be very sensitive to various factors. These include the saturation period prior to the growth and the temperature uniformity inside the furnace. With a few additional refinements in the growth system and growth procedure, layers of good surface morphology could be achieved with good reproducibility. X-ray rocking curves carried out on these layers at AT&T Bell Labs, Murray Hills, and Wright Patterson Lab. Dayton, indicated a full width half maxima (FWHM) typically in the range of 30 - 55 arcsec. The smallest half width we have obtained so far is 16 arcsec.

Compositional analysis of the samples were carried out using energy dispersive x-ray analysis attached to an ISI SS-40 scanning electron microscope available in Mechanical Engineering department. The details of the analysis along with the list of all the samples grown by this technique are given in Refs. 11 and 12 (see Appendices A and B).

III OPTICAL CHARACTERIZATION OF UNDOPED GaSb AND GaInAsSb

A. LOW TEMPERATURE PL STUDIES OF UNDOPED GaSb and GaInAsSb

The PL spectra of the layers were examined up to a low temperature of 4.5K. Our PL set-up has a closed cycle refrigerator system which goes only up to a temperature of 10K. In GaSb and GaInAsSb, excitons have been found to provide the prominent radiative decay mechanisms and information on these can be obtained only at lower temperatures of 4.5K. Hence, 4.5K PL measurements were carried out at Wright Laboratory, WPAFB in collaboration with Dr. Hegde and Dr. Mitchel.

Low temperature PL study of GaSb is well documented in the literature. For a reference we compared our PL spectra of LPEE grown GaSb with corresponding LPE data in the literature. No major differences were noticed between the two spectra. Normally, GaSb PL spectra are characterized by four bound excitons (BE) and recombination at the neutral acceptor level (BA) with its weak longitudinal optical (LO) phonon replica(19-21). This acceptor level has been attributed to native lattice defects which is a combination of Ga vacancy and a Ga atom on Sb site (22-24). It is present in GaSb layers grown by all the techniques.

The PL spectra of the quaternary layers exhibit similar features to those described for GaSb, however fewer near band edge structures are seen. The samples of three different compositions of GaInAsSb labelled as α, β, γ were studied. The room temperature PL peak wavelengths of band edge related peaks of these samples ranged from 1.7 μm to 2.28 μm . 4.5K PL spectral characteristics of the quaternary layers have been summarized in references

12 and 13 (Appendices B & C). The peak energy position and full width at half maxima (FWHM) of each peak has been determined by a quantitative fit to the experimental PL spectra using sum of the Gaussian line distributions. The FWHM of the bound excitons for the quaternary alloys were in the range of 4-7 meV in β and γ layers at 4K. These are the smallest line-widths reported for GaInAsSb on GaSb reported so far. A definite trend in the overall PL spectra is seen with the shift in the composition towards InAs. The overall integrated intensity remains the same for GaSb, α and β layers, but decreases by almost a factor of five to ten for γ samples. Free exciton is seen only for α -23 sample, as a weak band centered at 764.96 meV on the high energy side of the spectrum. This is seen in both GaSb and quaternary layers only under the highest excitation level used. With the shift in the composition towards lower energy gap, the highest energy transition line identified as BE_1 becomes dominant. The other bound excitons and donor to acceptor transitions become weaker. For γ sample, the donor to acceptor transition line is detectable only under high magnification. This is consistent with the experimental observations (4,25) on the layers grown by other nonequilibrium techniques where only one peak is seen for layers with compositions closer to or inside the miscibility gap region.

The identity of all the above transitions were further confirmed from the PL intensity dependence of the incident laser intensity. The temperature dependence of the PL integrated intensity and band gap energies were also investigated in detail. With increase in temperature, the overall integrated emission intensity of the quaternary PL spectra gradually decreases, indicating the presence of non-radiative mechanisms of decay with low activation energies.

The temperature dependence of the band gap energies were fitted using the well-known Varshni's equation (26). In GaInAsSb layers the band to band transition was estimated from the binding energy of BE_1 . For GaSb the values of the empirical constants used to fit the Varshni's equation were in excellent agreement with the values reported by Camassel et al. (27). However, they were considerably larger for layers with compositions closer to GaSb which may be an indicative of the presence of high degree of disorder in these layers. In the temperature range of 100-300K, the linear portion of the plot exhibited a slope of ≈ -0.31 meV/K for the quaternary layers which compared well with the value of -0.35 meV/K for GaSb(27).

Line shape analysis was also carried out. For GaSb and quaternary samples all the PL peaks could be well fitted by sum of Gaussian line distributions at low temperatures. With rise in temperature the PL spectra become increasingly asymmetrical, and the asymmetry sets in around 25-35K range indicating the dominance of band to band transitions. The PL spectral shape of band to band transitions were analyzed using the simple model of Van Roosbroeck-Shockley equation. A good fit was obtained at higher energies, however at lower energies a good fit was obtained if exponential band edge was assumed.

At higher temperatures, the emission spectra are narrower than the analytical spectra on the high energy side of the emission spectra, as self absorption due to higher photon energy within the epilayer has not been taken into account. The value of E_g determined from this analysis was found to be $kT/2$ less than the PL peak energy suggesting the k-conservative nature of the recombination processes.

It may be noted that these low temperature PL data represent the first results on

GaInAsSb alloy system. The details of the results presented in this section has been accepted for publication in Phys. Rev. B and J. Appl. Phys. (see Appendices A & B).

B. Low Temperature PL Characterization of Liquid-Phase Electro-Epitaxially Grown Te-doped GaSb Layers

We have investigated the characteristics of the Te doped layers as a function of Te concentration. Te is known to form a shallow donor level, 3.6meV below the conduction band in GaSb. Melt grown Te-doped GaSb single crystal has been extensively studied by Russians(28-32). Most of the PL characteristics that have been reported are typically at two low temperatures 12K-18K and 70-80K ranges, respectively. There has not been any mention on the FWHM of any of these PL peaks. However the PL spectral shape appear to be broad with FWHM around 30meV. Te doping leads to the introduction of a few deep impurity levels which are acceptor like and hence has led to some confusion in the identity of these levels. In Te doped GaSb, recombinations involving neutral residual acceptors A (34meV), ionized residual acceptors A^- (70-120meV)(29,30) deep acceptor C (28,29)(65-100meV) attributed to the donor - residual acceptor complex formation ($V_{Ga}Ga_{Sb}Te_{Sb}$), another deep acceptor D (130 meV the origin of which is not yet clearly understood) have been reported. A similar line corresponding to the recombination level at 65 meV (B) is also observed in the luminescence spectra of other III-V compound materials GaInSb(33,34), and GaAlSb(35).

In lightly doped Te -doped materials transition A is dominant and a few band edge transitions are seen sometimes accompanied with their phonon replica (29,30). With increasing compensation, A vanishes and transitions corresponding to C and A^- (28,29) appear. With very high Te doping levels the transition A^- also disappears and only the transition C is seen with the appearance of transition D at low excitation levels (29). Kyuregyan et al.(29) has reported a shift in these levels with the doping. However, its characteristics is not yet known in the alloy system.

Though the binary layers have been studied extensively, there is a lot of confusion as to the identity of the various levels. None of their studies include all the PL discussed. Hence, we have attempted to carry out a systematic and quantitative evaluation of the effects of Te compensation in GaSb examined under both low and high excitation conditions. We have grown both Te-doped GaSb and quaternary layers. However, analysis has been carried out only on doped GaSb layers.

Doped layers of three different Te concentrations have been grown. The carrier concentrations in these layers have not yet been determined. Depending on the amount of Te added to the melt we refer to them as heavily , moderately and lightly doped layers and the corresponding samples are labelled by H,M and L extension at the end of the sample name. The energy positions and the line widths at half maximum (FWHM) of each peak have been determined by a quantitative fit to the experimental PL spectra using a sum of Gaussian line distributions as described earlier in the preceding section . Due to the complicated nature of the experimental spectra, the dominant peaks were fit first with the additional peaks added as necessary.

The PL features found in our work under high excitation conditions are summarized and compared to our LPEE grown undoped GaSb in Table I. Several bound exciton-related

TABLE I Comparison of low temperature PL characteristics of Te-doped GaSb with undoped GaSb (Lee et al.(36) and our work(13)). Relative intensity is denoted by Rel. Int.

	Ref (36)	Ref (13)	AK-4		AK-9		F-8	
Identity	Energy (meV)	Energy (meV)	Energy (meV)	Rel.Int.	Energy (meV)	Rel.Int.	Energy (meV)	Rel. Int.
FE	810	808.5						
UI	808.7							
UI	808.0							
BE ₁	805.4	805.4			804	0.07	804	0.03
BE ₂	803.4	802.2						
BE ₃	800.1	799.1	801	0.16	800	0.01		
BE ₄	796.1	795.8	794	0.05	796	0.07	796	0.14
UI	795							
UI		784.8	787	0.16	790	0.56	789	0.06
							781	0.03
A	777.5	777.5	777	0.06	779	0.26	778	0.05
BE ₄ -LO	765	765.5						
B	758	756.3	757	1.00	756	0.61	758	1.00
UI	752							
A-LO	748.5	748.2						
C			743	0.98	744	1.00	744	0.71
D	728				725	0.16	725	0.41
UI	722							
A ⁻	710		713	0.15	714	0.43	710	0.10
UI	694						697	0.07
A ⁻ -LO	682				688	0.09	682	0.05
UI	680							

A band-residual acceptor transition

B band-acceptor transition

C band-acceptor transition (Te-related)

D band-acceptor transition (Te-related)

A⁻ doubly ionized acceptor level

transitions were seen only under high excitation with BE_1 - BE_4 usually overlapping from 796-804 meV. The shallow native residual acceptor transition (A), at 34 meV above the valence band, is still seen, but it is relatively insignificant as compared to the undoped result where it is the dominant feature. In addition, the corresponding deep acceptor level (A^-) is also present of an energetic value of 97 meV above the valence band. These values agree closely with our result on LPEE grown undoped GaSb (13).

Another dominant band-acceptor transition (B) occurs at 54 meV above the valence band which is in agreement with the value reported in literature for undoped GaSb (21). This peak is only present under high excitation as seen in Fig.3. The dominant peak (C) under both high and low excitation is seen at 744 meV, or 67 meV above the valence band, which is not present in undoped GaSb. Therefore, this peak most likely corresponds to a Te-related acceptor level as seen in Lebedev and Stel'nikova(28) and Kyuregyua et. al.(29). Several investigators have found a low intensity peak at 748 meV in undoped GaSb which has been attributed to a longitudinal optical (LO) phonon(13,36-38) but this peak, if present, is marked by the dominant peak at 744 meV.

Additional unresolved features we observed include another possible Te-related deep acceptor level at 725-731 meV (80-86 meV above the valence band) as well as some PL features between 777 (A) and 796 (BE_4) meV which we will refer to as UI. This is very close to the bound exciton peaks and, therefore, the transition involved is unclear. We also observe some additional deep levels which are more prominent under low excitation at 682-697 meV. These levels do not appear to vary significantly with doping level or input intensity, but may correspond to the deep acceptor level reported by Kyuregyan et. al.(29).

Spectral distributions undergo considerable change with excitation intensity in accordance with those reported in literature(29,39). When the excitation intensity is decreased by approximately an order of magnitude high energy transitions namely the excitonic transitions and shallow level transitions either become weak or disappear with the presence of additional new transitions at lower energies. In our work, the C peak dominates under low excitation with the deeper level A^- and D peaks also present. This may be explained by the fact that at higher intensity there is an increased compensation of the deep acceptor level caused by the enhanced excess carriers generated, thus increasing the probability of the higher energy transitions. Variation of output integrated intensity with the excitation intensity exhibited a slope of 0.7-1.1 range in the log-log plot for all the acceptors further confirming the assignment of the acceptor related transitions.

The identity of the bound exciton transitions were also confirmed from the temperature dependence. The variation of the integrated intensity with temperature at low intensity as shown in Fig.4 were fitted using the three level Boltzmann distribution developed by Bimberg et al.(40)

$$I_T/I_0 = 1 / \{1 + C_1 \exp(-\Delta E_1/kT) + C_2 \exp(-\Delta E_2/kT)\}, \quad (1)$$

where I_T/I_0 represents the normalized integrated intensity at 4.5K, ΔE_1 and ΔE_2 represent the effective mass donor binding energy and dissociation energy of the bound exciton, respectively, C_1 and C_2 are constants and are functions of the density of states. The values of C_1 and C_2 were determined to be around 1.01 and 2064 in excellent agreement with the undoped layers. However, the values of ΔE_1 and ΔE_2 were found to be around 2.1 meV and 27 meV, respectively, considerably higher than 1.1 and 10 meV computed in undoped LPEE layers (12).

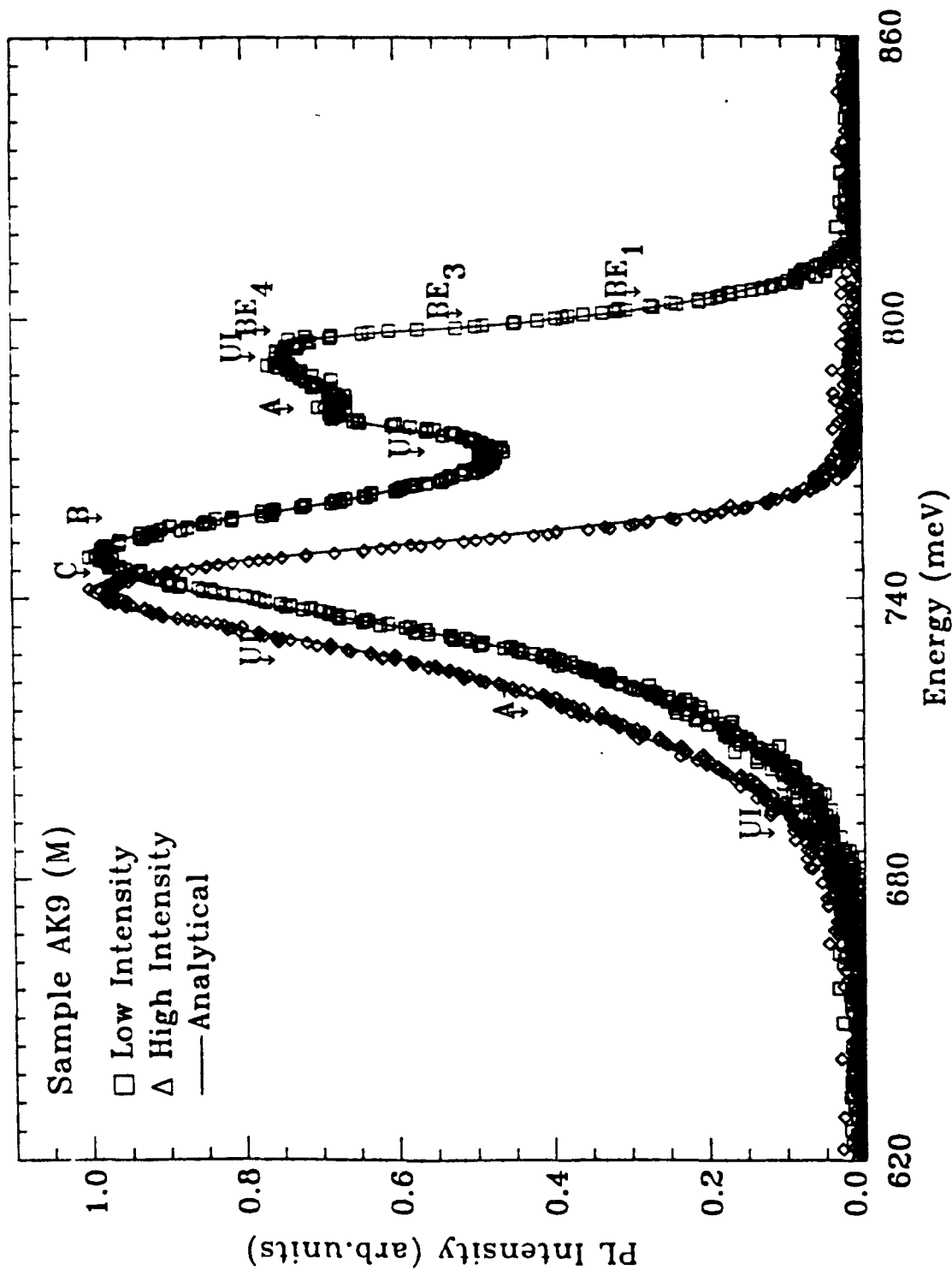


Figure 3. PL spectra of Te-doped GaSb at two levels of excitation intensity. High intensity refers to the spectra which is an order of magnitude higher than the intensity referred to as "low intensity". Solid lines represents the analytical spectra. The spectra is normalized with respect to the dominant peak in each of the layers.

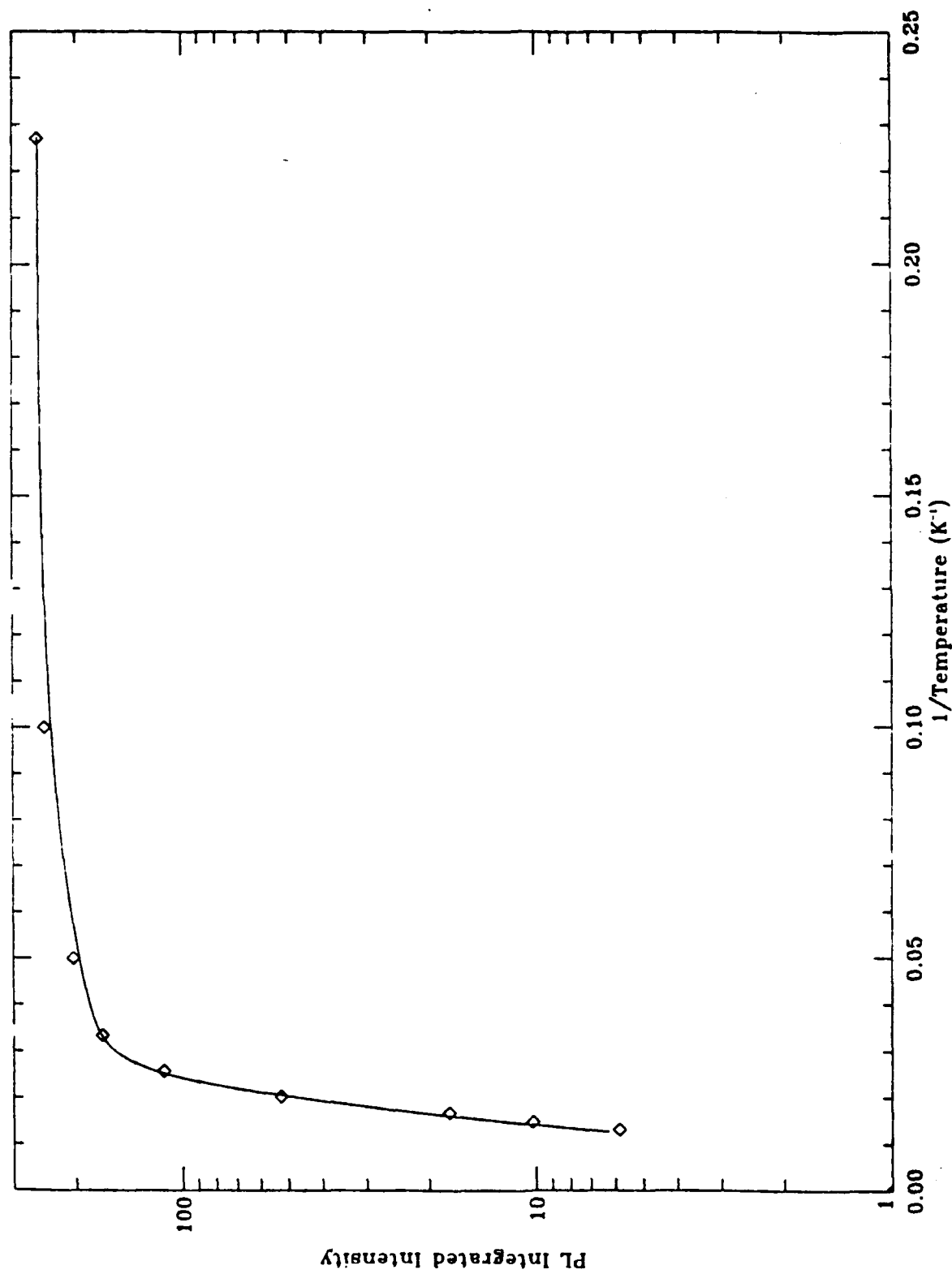


Figure 4. Analytical fit to the temperature dependence of integrated intensity of the deeper bound exciton transition (BE_3) at low temperatures.

The reason for this behavior is not clear at this time. Finally no shift in the peak positions were noticed in the intensity range investigated contrary to the reports of Lazareva and Stuchbnikov (32).

With increasing Te concentration, the transition due to the native acceptor level A dominant in undoped layers becomes small and transition due to the Te-related acceptor level (C) becoming prominent under low excitation (as seen in Fig.5). The transition at the deep level of the doubly ionizable acceptor A^- also starts increasing reaching its maxima at intermediate doping level before decreasing again at higher Te concentrations (see Fig.5). In addition, under high excitation conditions, the other native acceptor level (B) which is not reported in literature in Te -doped samples becomes prominent. It shows a complimentary behavior to the A^- transition becoming dominant at both low and high Te concentrations and decreasing for the intermediate range of concentrations (see Fig.5). These observations differ from those reported by Lebedev and Stel'nikova(28). They observe a systematic change in the dominance of the peak from native acceptor (A) in undoped to the Te-related acceptor level (C) at intermediate doping concentrations, and, finally, to the deep level of the doubly ionizable acceptor at the highest Te concentration. In addition they notice a shift in the PL peak energy with increasing Te concentration again contrary to our observations. It is possible perhaps our samples fall within the intermediate doping range used in the Lebedev et al.(28) study. Finally, the unidentified transition between 785-790 meV (UI) reaches its maximum value at the intermediate Te concentrations before decreasing again at high concentrations. Perhaps, as the electron concentration increases, the negatively charged ions are shielded forming a repulsive Coulombic barrier which screens the shallow acceptors at the highest Te concentrations.

In summary, the major PL features found in our study can be described using the proposed band diagram in Fig.6. We observe a doubly ionizable native residual acceptor (A/A^-) with shallow and deep levels at 34 meV and 97 meV, respectively, another native acceptor level for GaSb (B) is seen at 54 meV, and two Te-related acceptor levels (C&D) are found at 68 and 83 meV, respectively. In addition to these a few Te -related deep levels are also seen between 21-26 meV at higher Te concentrations. The relative dominance of each of these transitions are dependent on the degree of Te compensation in the layers and the incident excitation intensity. Finally, the bound excitonic transitions are described under the heaviest doping conditions which indicates good crystal quality. The limited temperature dependence and excitation intensity dependence data on output integrated intensity further confirms the nature of the transitions.

C. PHOTOREFLECTANCE

The experimental arrangement for photoreflectance is shown schematically in Fig.7. Light from a 100 W tungsten-halogen source was dispersed through a monochromator and was focused on the sample by means of two lenses. The reflected light was focused onto a silicon detector. An Argon-ion (4880A) laser was used as a pump beam and neutral density filters were used to reduce the laser power to about 100mW/cm². A beam expander was utilized to increase the laser spot size. The laser was focused onto the same spot as the monochromatic light on the sample, typical spot size was 10 mm x 1.0 mm. By chopping the laser beam at 200 Hz, the crystal's reflectivity is modulated periodically, and the signal was detected using the conventional lock-in techniques. To avoid self-modulation by the probe due to the variation in lamp-source intensity

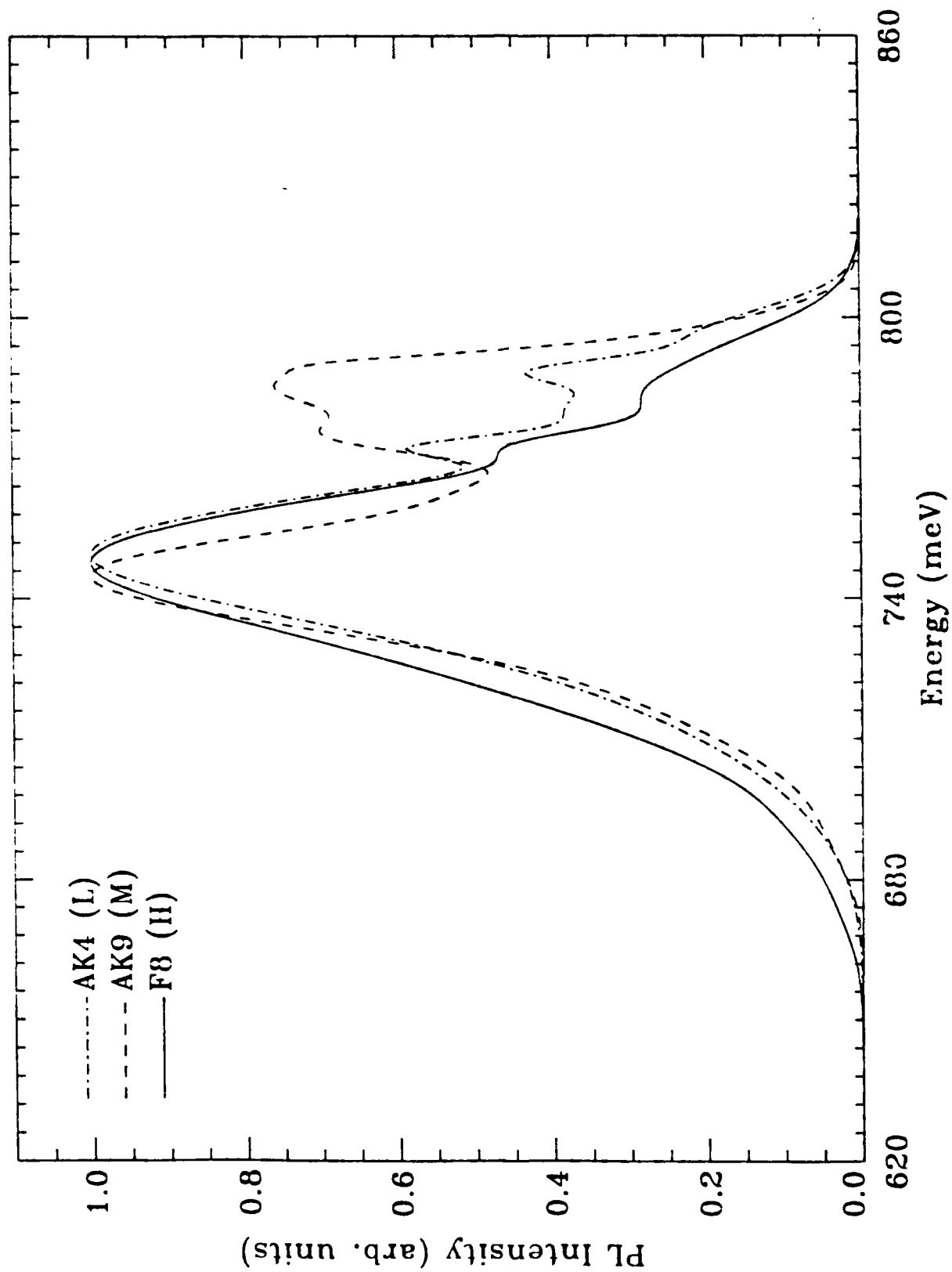


Figure 5. Variation of PL spectra with Te concentration in GaSb. The spectra is normalized with respect to the dominant peak in each of the layers.

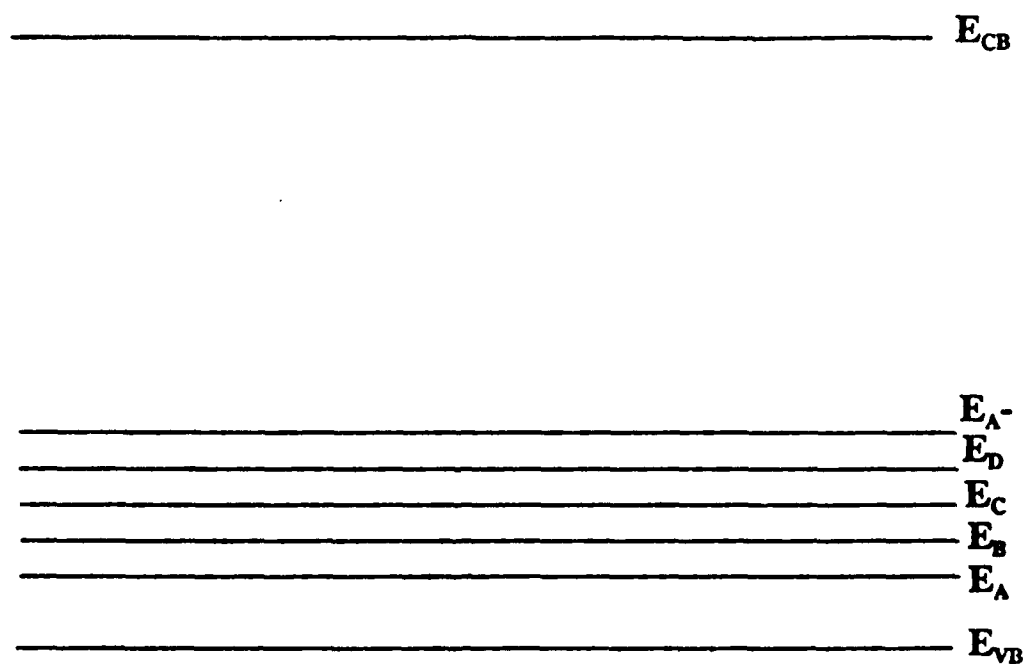


Figure 6. Energy band diagram of Te-doped GaSb at 4.5K, where E_{CB} =conduction band, E_{VB} =valence band, E_A =neutral residual acceptor, E_B =another neutral residual acceptor, E_C = Te related deep acceptor, E_D =another Te related deep acceptor, E_{A^-} =singly ionized level of residual acceptor A.

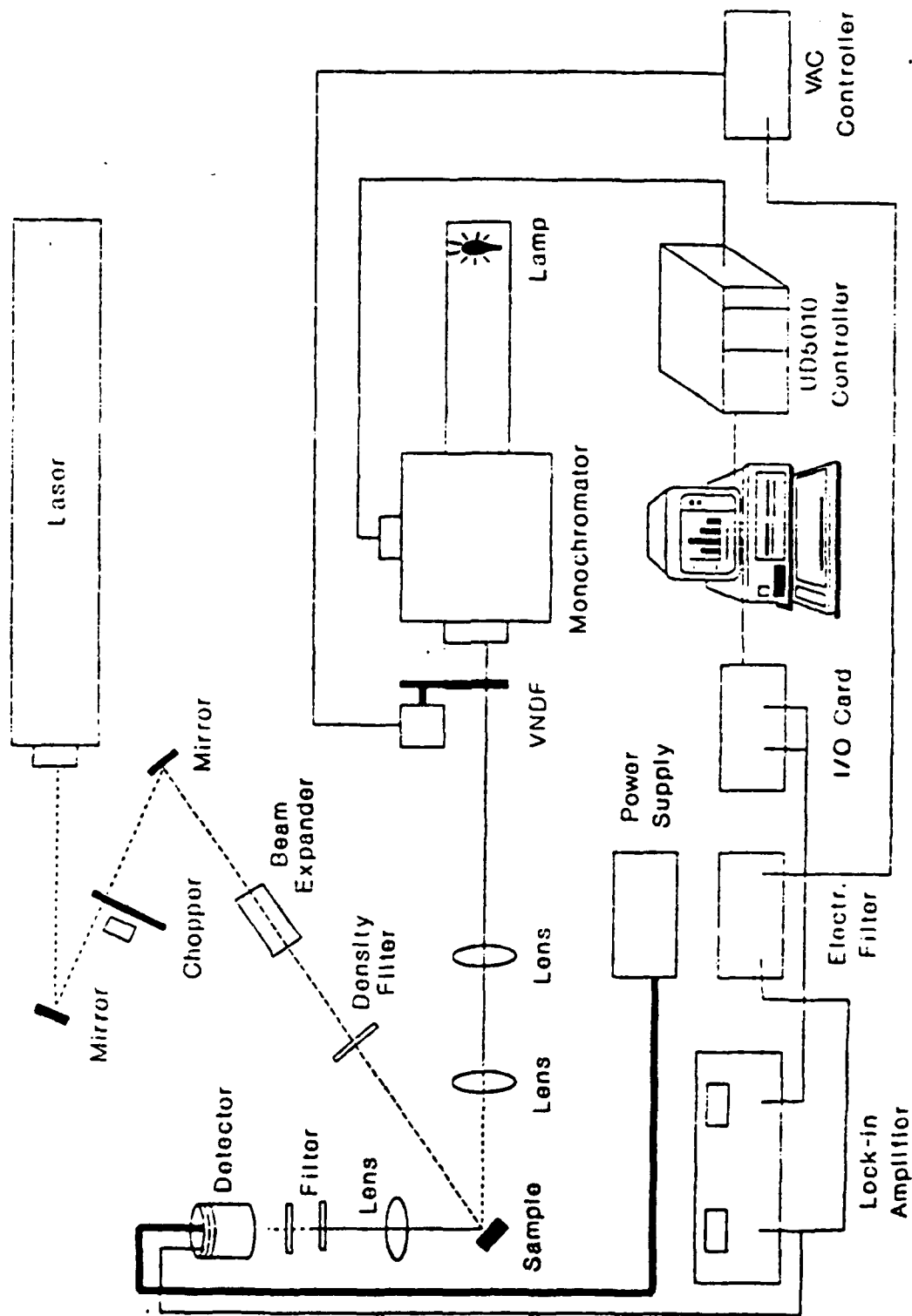


Figure 7. Schematic representation of a photorefectance experimental arrangement.

with wavelength, the dc component of the reflected signal was monitored and held constant by means of a variable neutral density filter placed in the optical path between the monochromator and the sample. The filter was driven by a stepper motor which was controlled electronically by the Compumotor Velocity and Acceleration card. This normalization procedure automatically corrects for any fluctuations in the reflected intensity due to the changes in the light intensity and variations on the surface of the sample. Two filters placed in front of the detector prevented the scattered laser entering the detector.

Figure 8 shows the PR spectra of a GaAs/AlGaAs HEMT structure obtained at Wright Laboratory, and in our laboratory. The resolution needs to be considerably improved. PR spectra was also obtained on semi-insulating GaAs samples indicating that the system is operational. However, no PR spectra were obtained in GaSb and GaInAsSb samples. This was also verified at Wright Patterson Laboratory. The system needs to be considerably modified.

IV GaInAsSb/GaSb PHOTODIODE

One of the main application of the GaSb semiconductor is in the optoelectronic devices. However, to realize this potential fully much needs to be done to understand the properties of the basic units of electronic devices, namely p-n junctions and Schottky diodes on GaSb. Our efforts were concentrated towards the fabrication of p-n junctions.

The Te-doped layers were grown on n-type substrate by LPEE. Typical layer thickness were around 2 μm . The patterns of 200 μm circular dots were defined using standard photolithography techniques. No mesa diodes were defined. The ohmic contacts to the substrate were accomplished by electroplating Au-Sn layers. On the epilayers, Au-Zn layer was electroplated. The contacts were then annealed at 350°C for 5-10 seconds in H_2 ambient.

The p-layer of the device was formed by the diffused Zn from the contacts. The I-V characteristic of the layers (see Fig.9) indicated a soft breakdown at a reverse bias of 800 mV (not shown in the Fig.9). C-V characteristics were determined using Materials Development Corporation doping profiler. The linear dependence of $1/C^2$ vs V as shown in the Fig.10. indicates the abrupt nature of the junction, the carrier concentration for this heavily doped sample has been determined to be about $1 \times 10^{17} / \text{cm}^3$. It is noteworthy that no mesa patterns were defined. Detailed characterization of these devices would be the focus of future research interest.

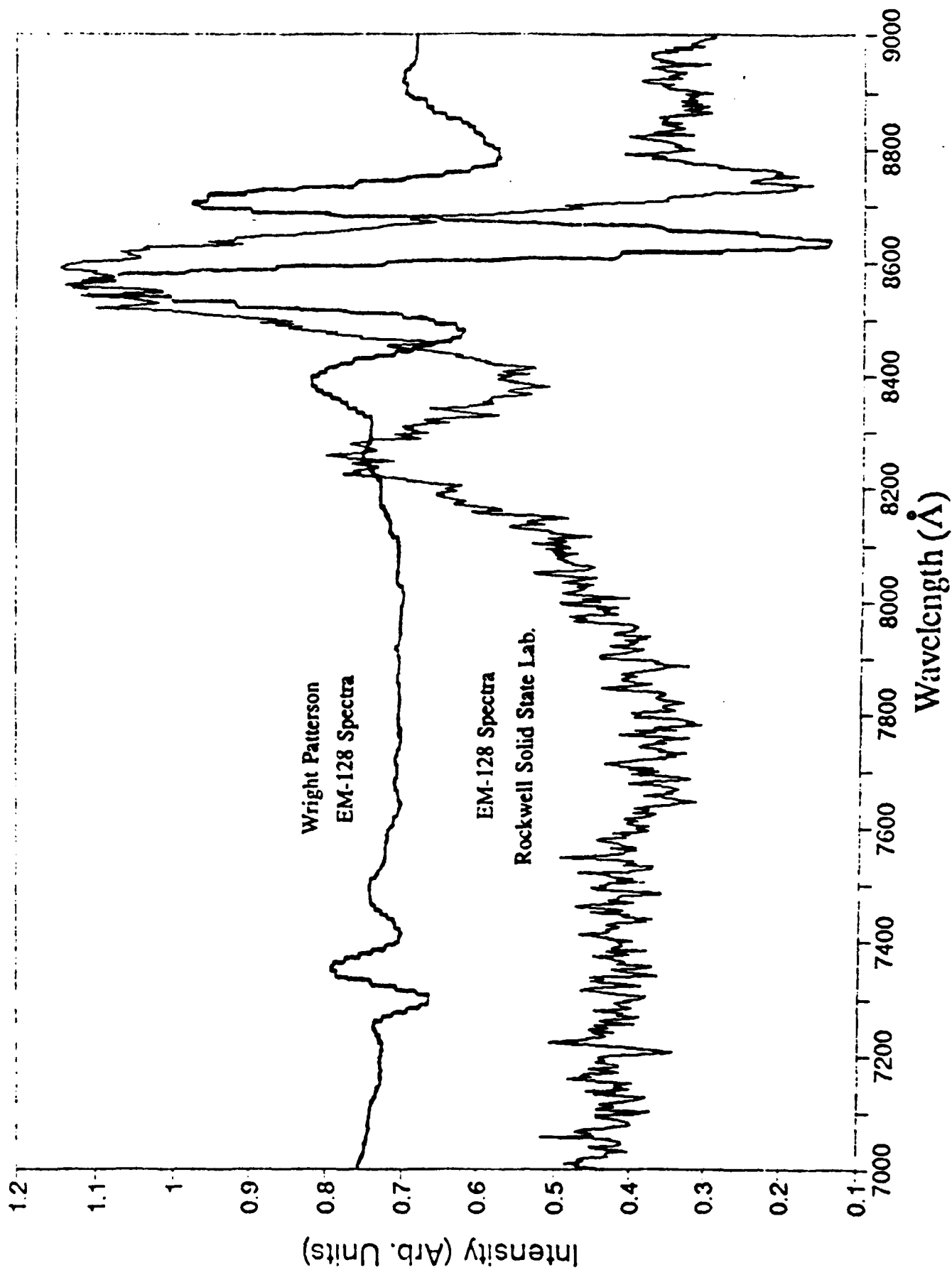


Figure 8. Comparison of PR spectra of EM-128 acquired at Wright Patterson and Rockwell Solid State Lab.

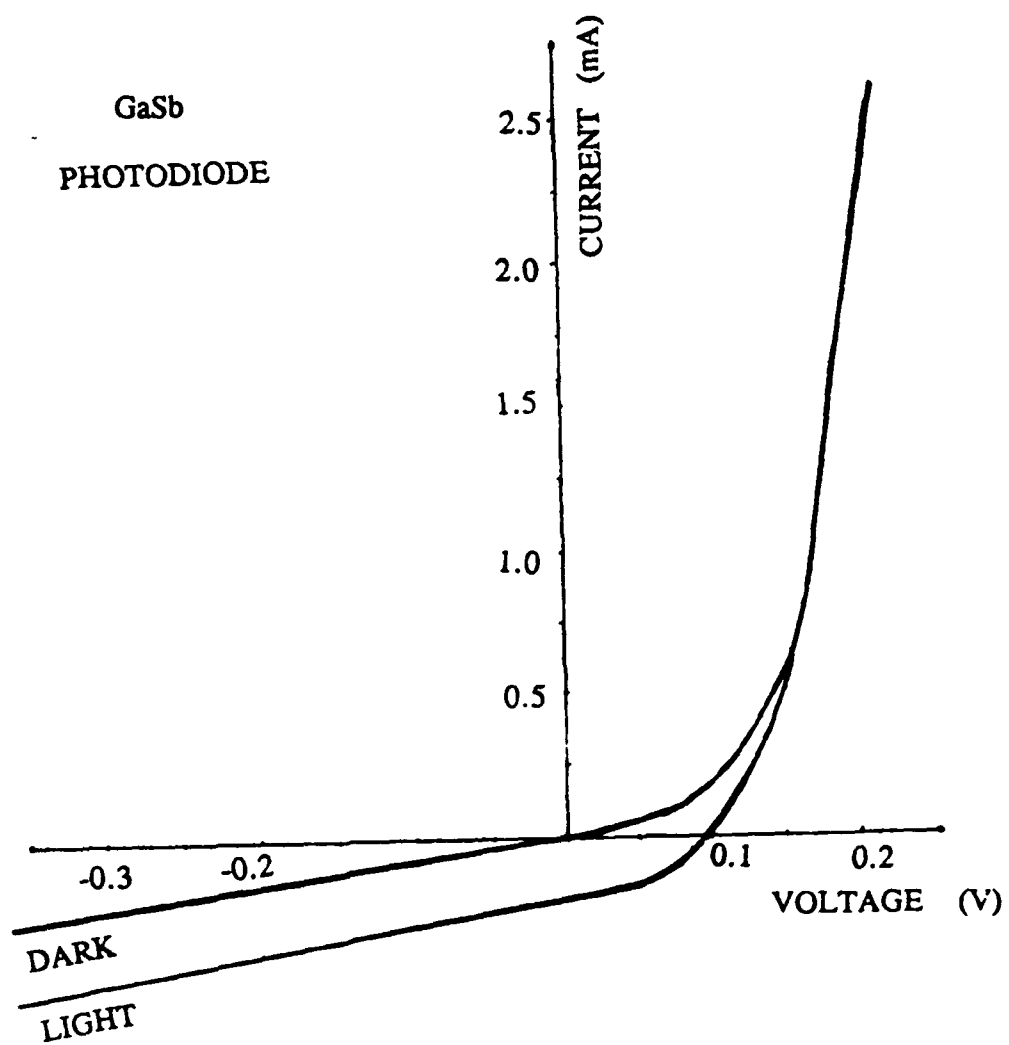


Figure 9. I-V characteristics of GaSb photodiode.

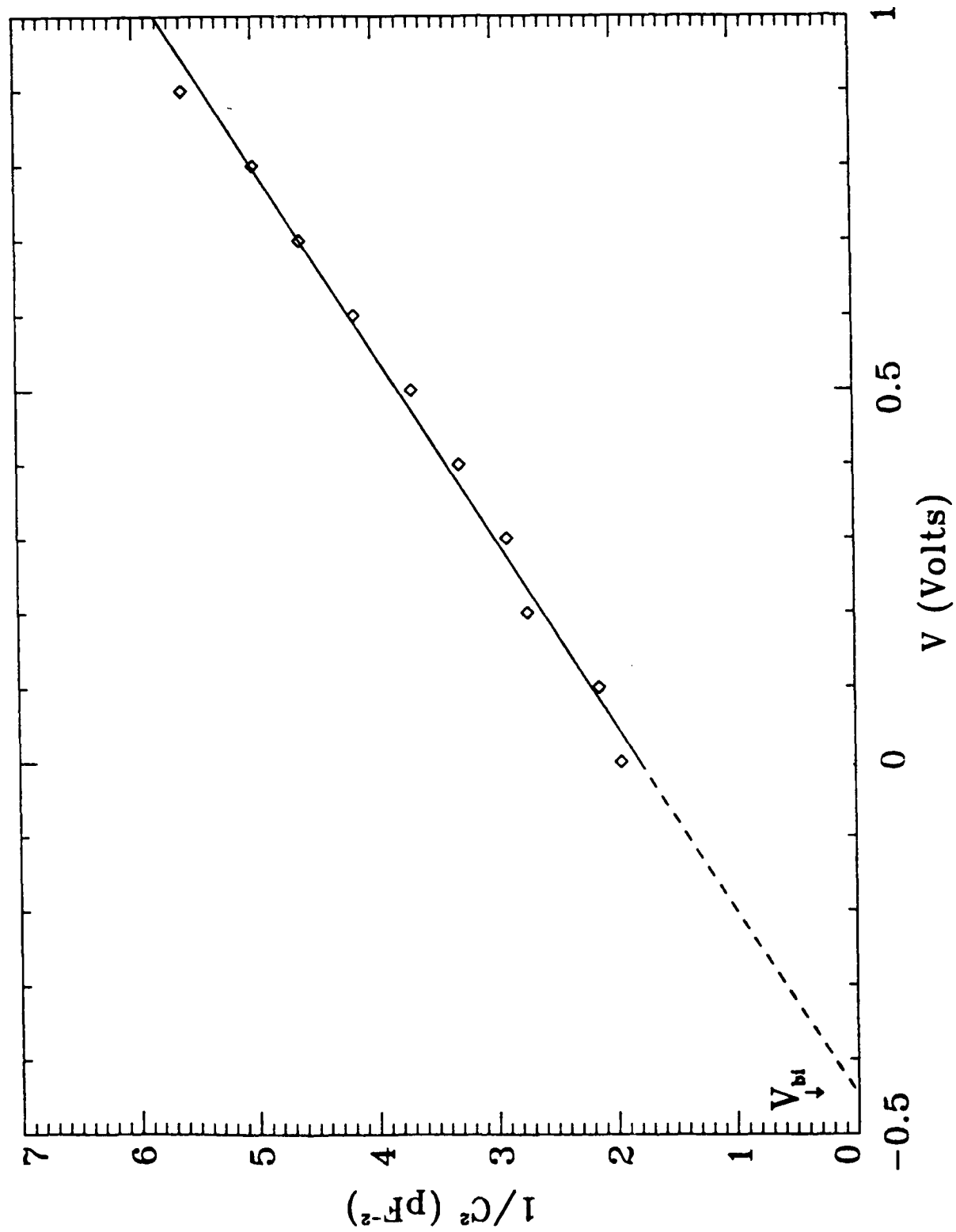


Figure 10. $1/C^2$ vs V of GaSb photodiode.

V BIBLIOGRAPHY

1. T.H. Chiu, J.L. Zyskind and W.T. Tsang, *J. Electron. Mat.* **16**, 57(1987).
2. W.T. Tsang, T.H. Chiu, D.W. Kisker and J.A. Ditzenberger, *Appl. Phys. Lett.* **46**, 283 (1985).
3. M.J. Cherng, H.R. Jen, C.A. Larsen, G.B. Stringfellow, H. Lundt and P.C. Taylor, *J. Cryst. Growth* **77**, 408 (1986).
4. M.J. Cherng, G.B. Stringfellow, D.W. Kisker, A.K. Srivastava and J. L. Zyskind, *Appl. Phys. Lett.* **48**, 419 (1986).
5. J.C. DeWinter, M.A. Pollack, A.K. Srivastava and J.L. Zyskind, *J. Electron. Mat.* **14**, 729 (1985).
6. A. Joullie, F. Jia Hua, F. Karouta and H. Mani, *J. Cryst. Growth* **75**, 309 (1986).
7. M. Astles, H.Hill, A.J. Williams, P.J. Wright and M.L. Young, *J. Electron. Material* **15**, 41 (1986).
8. R.Sankaran and G.A. Antypas, *J. Cryst. Growth* **36**, 198 (1976).
9. E. R. Gertner, A.M. Andrews, L.O. Bubulac, D.T. Cheung, M. J. Ludowise and R. A. Riedel, *J. Electron. Mater.* **8**, 545 (1979).
10. N. Kobayashi and Y. Horikoshi, *Jpn. J. Appl. Phys.* **20**, 2253 (1981).
11. Shanthi N. Iyer, Ali Abul-Fadl, Albert T. Macrander, Jonathan H. Lewis, Ward J. Collis and James W. Sulhoff, *Mat. Res. Symp. Proc.* **160**, 445 (1990).
12. Shanthi N. Iyer, S. Hegde, A. Abul-Fadl and W. Mitchel, *Phys. Rev. B* (in print)
13. S. Iyer, S. Hegde, K. K. Bajaj, A. Abul-Fadl, and W. Mitchel, *J. Appl. Phys.* (in print)
14. G.B. Stringfellow, *J. Cryst. Growth* **58**, 194 (1982).
15. A. Okamoto, J. Lagowski and H.C. Gatos, *J. Appl. Phys.* **53**, 1706 (1982).
16. Y. Imamura, L. Jastrzebski and H.C. Gatos, *J. Electrochem. Soc.* **125**, 1560 (1978).
17. J.J. Daniele and A. Lewis, *J. Electron. Mater.* **12**, 1015 (1983).
18. J. J. Daniele and A. J. Hebling, *J. Appl. Phys.* **52**, 4325 (1981).
19. W. Ruhle and D. Bimberg, *Phys. Rev. B* **12**, 2382 (1975).
20. W. Ruhle, W. Jakowetz, C. Wolk, R. Linnebach and M. Pilkuhn, *Phys. Stat. Sol. (B)* **73**, 255 (1976).
21. C. Benoit a la Guillaume and P. Lavallard, *Phys. Rev. B* **5**, 4900 (1972).
22. M.H. van Maaren, *J. Phys. Chem. Solids* **27**, 472 (1966).
23. Y.J. Van Der Meulen, *J. Phys. Chem. Solids* **28**, 25 (1967).
24. C. Anayama, T. Tanahashi, H. Kuwatsuka, S. Nishiyama, S. Isozumi and K. Nakajima, *Appl. Phys. Lett.* **56**, 239 (1990).
25. S.J. Eglash and H.K. Choi, *Gallium Arsenide and Related Compounds*, 1991, edited by G.B. Stringfellow (IOP, New York 1992) p.487.
26. Y.P. Varshi, *Physica* **34**, 149 (1967)
27. J. Camassel and D. Auvergene, *Phys. Rev. B* **12**, 3258 (1975).
28. A. I. Lebedev and I. A. Stel'nikova, *Sov. Phys. Semicond.* **13**, 29 (1979).
29. A. S. Kyuregyan, I. K. Lazareva, V. M. Stuhebnikov, and A. E. Yunovich, *Sov. Phys. Semicond.* **6**, 208 (1972).
30. A. A. Kastal'skii, S. B. Mal'tsev, and Y. G. Shreter, *Sov. Phys. Semicond.* **5**, 1360 (1972).

31. Y. E. Pokrovskii, K. I. Svistunova, and A.S. Kaminskii, *Sov. Phys. Semicond.* **1**, 26 (1967).
32. I. K. Lazareva and V. M. Stuchebnikov, *Sov. Phys. Semicond.* **4**, 550 (1970).
33. A.I. Lebedev and I.A. Strel'nilova, and A.E. Yunovich, *Sov. Phys. Semicond.*, **10**, 773, (1976).
34. A.I. Lebedev, I.A. Strel'nikova and A.E. Yunovich, *Sov. Phys. Semicond.* **11**, 1246, (1977).
35. A.N. Imenkov, T.P. Lideikis, B.V. Tsarenkov, Yu.M. Shernyakov, and Yu. P. Yakovlev, *Sov. Phys-Semicond.* **10**, 748 (1976)
36. M. Lee, D.J. Nicholas, K.E. Singer and B. Hamilton, *J. Appl. Phys.* **59**, 2895 (1986).
37. M. C. Wu, C. W. Chen, and C. C. Chen, *J. Appl. Phys.* **72**, 1101 (1992)
38. S. C. Chen and Y. K. Su, *J. Appl. Phys.* **66**, 350 (1989).
39. A. A. Kastal'skii, E. S. Filatova, and Y. G. Shreter, *Sov. Phys. Semicond.* **3**, 134 (1969).
40. D. Bimberg, M. Sondergeld and E. Grobe, *Phys. Rev. B* **4**, 3451 (1971).

VI. PUBLICATIONS & THESIS ARISING FROM AFOSR

Refereed Publications

1. Shanthi N. Iyer, Ali Abul-Fadl, Albert T. Macrander, Jonathan H. Lewis, Ward J. Collis and James W. Sulhoff, "Liquid Phase Electroepitaxial (LPEE) Growth of GaSb and GaInAsSb", MRS Symp. Proc. Vol.160, 445 (1990).
2. Shanthi N. Iyer, S. Hegde, A. Abul-Fadl, K.K. Bajaj and W. Mitchel, "Growth and Photoluminescence of GaSb & $Ga_{1-x}In_xAs_ySb_{1-y}$ Grown on Gasb substrates by Liquid-Phase Electroepitaxy", Phys. Rev.B (in print), (submitted for presentation in MRS Spring Meeting 1993)
3. Shanthi N.Iyer, S.Hegde, K.K.Bajaj, A.Abul-Fadl, and W.Mitchel, "Photoluminescence Study of Liquid Phase Electroepitaxially Grown GaInAsSb On (100) GaSb" J. of App. Phys.(accepted for publication),(submitted for presentation in APS Spring Meeting 1993).

Non-refereed Publications and Presentations

1. S. Iyer, "LPEE Growth & Characterization of GaInAsSb", 1st HBCU Meeting on PMMS' 90, Howard University, Washington, May 16, (1990)
2. Jonathan Lewis, S. Iyer, Ali Abul-Fadl and W.Collis, "Liquid Phase Electroepitaxial Growth and Characterization of InGaAsSb lattice Matched to (100) GaSb in the 1.7 to $2.3\mu m$ ", Proc. of 1st Annual Symposium on CSA, Greensboro, NC, p.57 (1990).
3. S. Iyer, A. Abul-Fadl, S. Vaddi, and W.J. Collis, "Photoluminescence Study of LPEE Grown GaInAsSb Epilayers on GaSb", Proc. of 2nd Annual Symposium on CSA, Greensboro, NC, p.53-6 (1991).
4. R. Cardona, S. Iyer, and A. Abul-Fadl, "Photoreflectance as an Optical Characterization Tool", ibid., p.58 (1991).
5. S. Vaddi, S Iyer and A. Abul-Fadl, "LPEE Growth of GaInAsSb System", ibid., p.108-109 (1991).
6. C. Durham, A. Abul-Fadl, and S. Iyer, "Photoluminescence/Photoreflectance Data Acquisition", ibid., p.106-107 (1991).
7. L. Small, "Photoluminescence Spectral Analysis of GaInAsSb Semiconductor Layers", IEEE Southeast Con., (1992)
8. D.L. Simpson, S. Iyer, and A. Abul-Fadl, "Liquid Phase Electroepitaxial (LPEE) Growth and Photoluminescence Characterization of Undoped GaInAsSb ($2.25\mu m$) at $530^\circ C$ ibid, p. 525-6 (1992)
9. L. Small and S. Iyer, "Photoluminescence Spectral Analysis of GaInAsSb Semiconductor Layers", ibid, p.527-30 (1992)
10. S. Iyer, "LPEE Growth & Photoluminescence Characteristics of GaSb & GaInAsSb alloys", Wright Patterson Laboratory, June (1991)
11. S. Iyer, "LPEE Growth & Characteristics of GaInAsSb alloys", Emory University, Feb. 27 (1992)

Publication in preparation

1. "Photoluminescence Study of LPEE Grown Te-doped GaSb and GaInAsSb on (100) GaSb" by S.Iyer et al.

Undergraduate Project

1. Lori Small, "Photoluminescence spectral analysis" , Dec. 1991.

Graduate Degrees Awarded

1. S. Vaddi, M.S.E.E. " Photoluminescence Study of LPEE Grown GaSb and GaInAsSb Layers on (100) GaSb", Dec. 1991.
2. D. Moxey, M.S.E.E. " LPEE Growth and Characterization of Te-Doped GaSb and GaInAsSb on (100) GaSb at 574°C", May 1992.
3. Rufino Cardona, M.S.E.E., "Photoreflectance characterization of semiconductors", August, 1992.

Master's Thesis in Progress

1. Darrell Simpson, "Growth of Te-doped GaSb & GaInAsSb for Device Applications".
2. Lori Small, "Photoluminescence characterization of LPEE grown Te doped GaSb and GaInAsSb"

APPENDIX A

MRS Symp.Proc.160,445(1990)

LIQUID PHASE ELECTROEPITAXIAL (LPEE) GROWTH OF GaSb AND GaInAsSb

Shanthi N. Iyer*, Ali Abul-Fadl*, Albert T. Macrander**, Jonathan H. Lewis*, Ward J. Collis * and James W. Sulhoff***
 *North Carolina A&T State University, Greensboro, NC 27411
 **AT&T Bell Laboratories, Murray Hill, NJ 07974
 ***AT&T Bell Laboratories, Short Hills, NJ 07733

ABSTRACT

Liquid phase electroepitaxial technique has been used for the growth of GaSb and GaInAsSb in the composition range corresponding to peak band gap wavelengths of 1.7-2.28 μ m. The growth rate of these layers were examined as a function of current density. The growth rates of these layers are typically 0.8 μ m/min. at a current density of 10A/cm². The quality of the layers was evaluated by x-ray diffraction and room temperature photoluminescence.

INTRODUCTION

GaInAsSb alloys lattice matched to GaSb are currently of great interest due to their potential applications in future optical communication system in 2-4 μ m range. However, this alloy system is known to have a large miscibility gap in the central region which limits the range of solid composition that can be grown by liquid phase epitaxy (LPE) [1-4]. Though layers inside the miscibility gap has been grown by MOVPE [5,6] and MBE [7,8], LPE technique is still believed to offer one of the best device quality layers. The liquid phase electroepitaxial (LPEE) technique differs from the conventional liquid phase epitaxy in that the growth is induced and sustained by a current that is passed through the melt-substrate interface. LPEE, unlike conventional LPE, is controlled by an external parameter independent of the furnace temperature and hence is expected to yield layers of improved surface morphology, better compositional homogeneity and interface stability [9-11].

In this paper, we report the first growth of GaSb and GaInAsSb layers on (100) GaSb by liquid phase electroepitaxial technique. The results of the characterization of these samples are presented.

EXPERIMENTAL

Ga_{1-x}In_xAs_ySb_{1-y} layers were grown in a hydrogen ambient in a horizontal slider boat system modified to permit the passage of current through the melt-substrate interface. The details of the growth system have been described elsewhere [12]. Undoped (100)-oriented GaSb wafers of thickness 0.4mm (16 mil) and an area of 6mmx6mm were used as substrates. The melt was prepared using In, Ga, undoped GaAs and GaSb, and In, undoped InSb, GaSb and GaAs as the source materials for compositions grown at 580°C

and 530°C, respectively. The liquidus composition of the melt was determined by conventional source dissolution technique. The layers were grown with excess GaSb floating on top of the melt which provided a constant source of Sb.

The lattice mismatch of the epilayers was determined either by double crystal x-ray diffraction or high resolution x-ray diffraction. In double crystal diffractometer rocking curves were measured for (400) Bragg reflection using CuK α radiation and a (100) InP first crystal. Photoluminescence measurements were carried out using the argon ion laser as the excitation source with a 3/4m monochromator and a InAs detector with conventional lock-in techniques for dispersion and detection purposes, respectively. The compositions of the layers have been determined by the energy dispersive spectrophotometer attached to an ISI SS-40 scanning electron microscope. GaSb, GaP and InAs binaries were used as the standards for Sb, Ga, In and As, respectively. The quantitative analysis was carried out using Tracor Northern computer. MICROQ program with ZAF correction was used to analyze the x-ray spectra.

RESULTS AND DISCUSSION

GaSb layers were grown at a growth temperature of 580°C. At this temperature however, we were able to grow quaternary layers of GaInAsSb only in the composition range corresponding to the wavelength range of 1.7 μ m to 1.99 μ m. No problems relating to oxidation of the substrate were observed, as has been reported in the literature [2]. The surface morphology of the layers was good, exhibiting slight terracing. For GaInAsSb layers of compositions closer to the miscibility gap, catastrophic dissolution of the substrate occurs at a temperature of 580°C due to the unstable melt. Hence, for the layers of the compositions corresponding to energy gaps of 0.55 eV and lower, the growth temperature was reduced to 530°C. These layers exhibited slightly rough surface and often oval features along [110] direction. The liquidus and solidus data for different compositions of grown layers are summarized in Table 1. Though the data is limited it may be noted that there appears to be a significant reduction in the distribution coefficient of As from 120 to 40 with increase in temperature from 530°C to 580°C. This observation is consistent with that of Drakin et al. [3]. Hence, as the distribution coefficient of As becomes comparable to that of other elements, it is expected that the layers grown at 580°C would exhibit better compositional homogeneity.

We have also examined the variation of growth rate with current density for these layers. The growth rate in conventional LPE is mainly diffusion limited, while in LPEE besides diffusion there are two mechanisms contributing to the solute transport towards the substrate-melt interface. These are electrotransport [13,14] and Peltier cooling [13,14]. The growth conditions may be suitably tailored so that one mechanism may dominate the other. In our case we have used thin substrates typically 16 mil thick to reduce the effect of Peltier cooling. The growth rate of GaSb layers increases somewhat linearly with the current density, as illustrated in Fig.1, indicating that the electrotransport is the dominant mechanism contributing to the growth process. The growth rate is typically 0.8 μ m/min at a current density of 10A/cm². The growth rate of the quaternary layers do not vary significantly from the binary. Layers in the thickness range of 1-10 μ m have been grown by this technique.

Figure 2 shows the x-ray rocking curves and room temperature

TABLE 1
SUMMARY OF GROWTH CONDITIONS
AND CHARACTERIZATION RESULTS

Liquid Composition			Growth Temp (°C)	Current Density (A/cm ²)	Thick- ness (μm)	A _g (μm)	E _g (eV)	ΔE _g (eV)	x	y
x ₁ In	x ₂ Ge	x ₃ As								
0.00000	0.88918	0.00000	580	1.4	6.5	1.698	0.732	0.000	0.000	0.000
0.1593	0.70094	0.00103	581	6.0	6.0	1.790 (0.694)	0.693 (0.068)	0.010 (0.068)	0.027	0.04
0.4288	0.33599	0.00156	572	7.5	3.7	1.991 (0.633)	0.624 (0.149)	1.042 (0.149)	0.065	0.178
c			572	7.5	7.0	-- (0.643)	-- (0.146)	1.089 (0.146)	0.059	0.067
0.52694	0.12210	0.00149	535	8.9	3.7	2.276 (0.567)	0.545 (0.567)	0.083 ^a (0.567)	0.16	0.04
c			535	12.1	7.0	-- (0.565)	-- (0.015)	-- (0.015)	0.02	0.171
c			535	14.4	7.0	-- (0.531)	-- (0.531)	1.055 ^a (0.531)	0.189	0.180
0.64217	0.08342	0.00834	529	10.0	5.6	-- (0.525)	-- (0.525)	-- (0.525)	0.055	0.154

c indicates that the samples were grown from consecutive runs from the previous one.
^a indicates that the lattice mismatch was determined by high resolution x-ray diffraction.
 The analytical values are given in the parentheses.

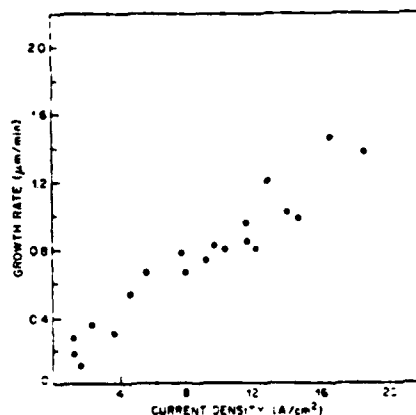


Fig.1. Dependence of growth rate on current density for GaSb epilayers.

photoluminescence (PL) spectrum of a sample with peak wavelength at 1.99μm, respectively. The full width at half maximum (FWHM) of the rocking curve for this sample is 27 arcsec, which is close to the half width of 20-25 arcsec normally seen on the substrate itself, indicating good crystalline quality and compositional homogeneity of the epilayers. Further, FWHM of PL spectrum of this sample is also low 35 meV confirming the above observations. Typically, the FWHM of x-ray rocking curves and PL spectra for different layers were found to lie in the range of 25-45 arcsec and 30-50 meV, respectively.

The compositions determined from energy dispersive x-ray analysis were used to estimate the room temperature lattice

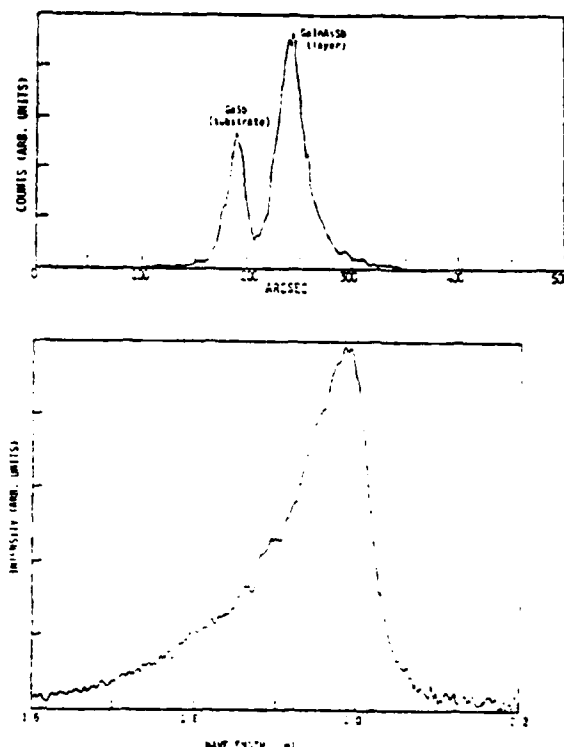


Fig.2. X-ray double crystal rocking curve of the (400) Bragg reflection and room temperature PL spectrum of the sample with peak wavelength at 1.99 μm .

mismatch between the quaternary epilayers and the substrate from Vegard's law. The computed values of the lattice mismatch are close to the experimental values, though exact agreement is not obtained as seen from Table 1. Further, the energy gaps were calculated using the interpolation scheme based on the weighted average of the binaries and the average bowing parameter weighted by the composition [1,15]. The discrepancy between the calculated and experimental values seems to increase for compositions towards the miscibility gap. This is in agreement with the observations of DeWinter et al. [1].

In summary, we have grown GaInAsSb layers in the composition range of $0 \leq x < 0.2$ by LPEE technique. The narrow PL and x-ray rocking curves attest to the good crystal quality of the epitaxial layers. Linearity of the growth rate versus current density indicates that the electrotransport is the dominant mechanism contributing to the growth process.

ACKNOWLEDGEMENTS

We would like to acknowledge the assistance of Ranjan Vaidyanathan for EDAX measurement. This work was supported by the AFOSR (Contract No. F 49620-89-C-0004).

REFERENCES

1. J.C. DeWinter, M.A. Pollack, A.K. Srivastava and J.L. Zyskind, *J. Electron. Mater.* **14**, 729 (1985).
2. M. Astles, H. Hill, A.J. Williams, P.J. Wright and M.L. Young, *J. Electron. Mater.* **14** (1985).
3. A.E. Drakin, Peter G. Eliseev, B.N. Sverdlov, A.E. Bochkarev, L.M. Dolginov and L.V. Druzhinina, *IEEE J. Quantum Electron* **QE-23**, 1089 (1987).
4. A. Joulie, F. Jia Hua, F. Krouta and H. Mani, *J. Cryst. Growth* **75**, 309 (1986).
5. M.J. Cherng, G.B. Stringfellow, D.W. Kisker, A.K. Srivastava and J.L. Zyskind, *Appl. Phys. Letter* **48**, 419 (1986).
6. M.J. Cherng, H.R. Jen, C.A. Larsen, G.B. Stringfellow, H. Lundt and P.C. Taylor, *J. Cryst. Growth* **77**, 408 (1986).
7. W.T. Tsang, T.H. Chiu, D.W. Kisker and J.A. Ditzenberger, *Appl. Phys. Lett.* **46**, 283 (1985).
8. T.H. Chiu, J.L. Zyskind and W.T. Tsang, *J. Electron. Mater.* **16**, 57 (1987).
9. J.J. Daniele and A. Lewis, *J. Electron. Mater.* **12**, 1015 (1983).
10. A. Okamoto, J. Lagowski and H.C. Gatos, *J. Appl. Phys.* **53**, 1706 (1982).
11. Y. Imamura, L. Jastrzebski and H.C. Gatos, *J. Electrochem. Soc.* **125**, 1560 (1978).
12. A. Abul-Fadl, E.K. Stefanakos and W.J. Collis, *J. Cryst. Growth* **11**, 559 (1982).
13. L. Jastrzebski, J. Lagowski, H.C. Gatos and A.F. Witt, *J. Appl. Phys.* **49**, 5901 (1978).
14. T. Bryskiewicz, J. Lagowski and H.C. Gatos, *J. Appl. Phys.* **51**, 988 (1980).
15. R.L. Moon, G.A. Antypas and L.W. James, *J. Electron. Mater.* **3**, 635 (1974).

APPENDIX B

Phys. Rev. B (in print)

**GROWTH & PHOTOLUMINESCENCE OF LIQUID PHASE
ELECTROEPITAXIALLY GROWN GaSb & $\text{Ga}_{1-x}\text{In}_x\text{As}_y\text{Sb}_{1-y}$ ON GaSb**

**S. Iyer
S. Hegde*
Ali Abul-Fadl
K.K. Bajaj**
W. Mitchel*****

**Department of Electrical Engineering
North Carolina A&T State University
Greensboro, NC 27411**

*** University of Dayton Research Institute
Dayton, OH 45469-0178**

**** Department of Physics, Emory University
Atlanta, GA 30322**

***** Materials Directorate, Wright Laboratory,
Wright Patterson Air Force Base, OH 45433-6533**

ABSTRACT

We report on the liquid phase electroepitaxial (LPEE) growth of GaSb and $\text{Ga}_{1-x}\text{In}_x\text{As}_y\text{Sb}_{1-y}$ alloys on undoped (100) GaSb substrates. Alloys with room temperature photoluminescence peak wavelengths as long as $2.32\ \mu\text{m}$ have been grown. These layers were assessed by x-ray diffraction, energy dispersive x-ray analysis and low temperature Fourier transform photoluminescence (PL) with emphasis on the latter. The variation in the low temperature photoluminescence bands as a function of the alloy composition has been investigated. The low temperature (4.5K) PL spectra of the alloys exhibited narrow peaks with full width half maxima in the range of 3-7 meV indicating an excellent quality of the LPEE grown epilayers. The temperature and intensity dependences of the PL spectra were investigated to identify the nature of the recombination processes.

PACS NOS. 78.55.Cr, 71.55. Eq, 71.35.+z, 81.15.Lm.

I INTRODUCTION

The quaternary alloys $\text{Ga}_{1-x}\text{In}_x\text{As}_y\text{Sb}_{1-y}$ are currently of great interest for use in infrared devices ($1.7\text{-}4.1\mu\text{m}$). The unique feature of this alloy system is the presence of the miscibility gap which covers almost the entire composition range at typical growth temperatures (Fig.1) Nonequilibrium techniques, namely, organometallic vapor phase epitaxy (OMVPE) (1,2) and molecular beam epitaxy (MBE) (3,4) have been successfully used for the growth of these layers in the miscibility gap region. The layers grown by liquid phase epitaxy (LPE) (5-10) are limited by the presence of the miscibility gap, and the composition with the longest wavelength reported inside the gap is $2.33\mu\text{m}$ (5), corresponding to x of 0.22 and y of 0.18 on GaSb substrates. For compositions away from the substrate corresponding to $x \geq 0.8$ (8,9) difficulties have been encountered due to the growth solutions tending to dissolve the substrate. Hence, most of the LPE work has been concentrated over a very narrow composition range, for $x < 0.25$ (5-7) on GaSb substrates and for $x \leq 0.2$ (7,8) and $x \geq 0.83$ (8,10) on InAs substrates.

Iyer et al.(11), have reported the growth of these layers lattice matched to GaSb by liquid phase electroepitaxial (LPEE) technique. In the LPEE technique unlike LPE, the growth is carried out at a constant furnace temperature and is induced and sustained by an external parameter, in this case, the current density. The advantages of LPEE over LPE grown layers in terms of the interface stability (12), surface morphology (13) and the compositional homogeneity (14,15) are well established. Epitaxial layers of InSb (16) were the first binary III-V semiconductor compound layers grown by this technique. However, since then GaAs

(13), InSb¹⁶, InP(17), GaP (18), InAs (19), Ga_{1-x}Al_xAs (15), InGaAs(20,21), InGaP (14) and Ga_{1-x}In_xAs_yP_{1-y} (22) have been grown by this technique.

GaSb, unlike other commonly known III-V semiconductors such as GaAs and InP, has a somewhat large concentration of residual acceptors. The dominant residual acceptor has been attributed to the native defect caused by Sb deficiency, predominantly either due to the Ga antisite(23) , or a Ga antisite in the vicinity of a Ga vacancy (24-26). The nature of this acceptor has been a subject of extensive studies to determine whether the residual acceptor is a single acceptor (24,27) or a double acceptor (28,39). The strong evidence of the latter has been shown in compensated materials (28,29), namely in donor-doped layers. The first and second ionization energy levels of this acceptor have been determined to be in the range 30-35meV (23,28,29) and 70-120 meV (28,30), respectively. In addition, another dominant acceptor level is present at 54 meV above the valence band in GaSb (27,31). However, the nature of this acceptor level is not well understood. Very little is known about the acceptors due to chemical impurities in this material.

The low temperature photoluminescence has so far been an important characterization tool for assessing the quality of GaSb layers. Due to the presence of different acceptor levels in this material, the low temperature PL spectra exhibit numerous transitions which include free excitons, recombinations at the different acceptor levels and excitons bound to these neutral acceptor levels. Hence, if the layers grown are not of high purity, there is a considerable misinterpretation of the origin of the PL peaks. The sharp structures near the band edge in GaSb have been attributed to excitons bound to different neutral acceptors (27,32,33). In high quality GaSb material, four bound excitons have been resolved (32,33) at low temperatures occurring

at 805.4, 803.4, 800.1 and 796.1 meV, respectively. They will be referred to as BE_1 , BE_2 , BE_3 & BE_4 , respectively following the nomenclature of Ruhle et al. (32), which is now commonly used. The binding energies of excitons to the acceptors are significantly different and much larger than commonly observed in other III-V semiconductors such as GaAs, InP & InSb. Both Johnson et al. (30) and Guillaume et al. (27) have identified BE_2 to correspond to an exciton bound to a native acceptor level at 34 meV, from Zeeman splitting and piezoemission experiments, respectively. The transition BE_4 has also been ascribed to an exciton bound to a neutral acceptor level (27,32) above the valence band from the piezoemission data (27). However, Johnson et al. (30) have suggested the possibility of this transition being due to an exciton bound to an ionized acceptor, while Pollak et al. (34) claimed to observe no splitting of the levels under uniaxial stress questioning the identity of the above transitions. The origin of the other two bound exciton transitions BE_1 and BE_3 is not yet clearly understood.

While there have been several reports on GaSb, there has been no detailed study of the radiative transitions in $Ga_{1-x}In_xAs_ySb_{1-y}$. As is well known for III-V semiconductor compounds and alloys in general, the properties of the material are growth specific. Hence, it becomes important to compare specific fundamental characteristics and the quality of the materials grown by LPEE technique with those grown using other techniques, in particular the LPE technique. In this work, we present a systematic study of the LPEE grown $Ga_{1-x}In_xAs_ySb_{1-y}$ layers of compositions corresponding to the room temperature wavelength in the range 1.7 μm to 2.28 μm . The results of the dependence of PL characteristics on the excitation laser power, temperature and the alloy composition are reported.

II EXPERIMENTAL DETAILS

A conventional horizontal slider boat system which was designed to allow the passage of current through the melt-substrate interface was used for the LPEE growth of $\text{Ga}_{1-x}\text{In}_x\text{As}_y\text{Sb}_{1-y}$. The details of the growth system and the growth procedure have been described elsewhere (11,20). Undoped (100) GaSb wafers of thickness 0.4mm (16 mil) and an area of 6mmx6mm were used as substrates. GaSb and three different compositions of the quaternary alloys were grown. The liquidus composition of the melt was determined by the source dissolution technique. Excess GaSb was added prior to epilayer growth to provide a continuous source of Sb. The lattice mismatch of the layers were determined either by double crystal x-ray diffraction or by high resolution x-ray diffraction. The rocking curves were recorded for the (400) reflection of $\text{CuK}\alpha$ line from an InP and Si monochromator crystals, respectively.

The low temperature PL spectra were obtained using a BOMEM fourier transform spectrometer at a resolution of 0.2 meV. An Ar-ion laser operating at 514.5nm provided the excitation source. The maximum output power was limited to 140 mW. The spectra were taken using a focused laser spot on the sample and a liquid nitrogen cooled InAs as the detector. The beam diameter on the sample was 100-500 μm and typical excitation power density on the sample was $\sim 1 \text{ W/cm}^2$. The low temperature measurements were carried out in a variable temperature continuous flow liquid helium cryostat. A different set up was used for recording the room temperature PL spectra. It consisted of a 0.5 m grating monochromator and a PbS detector with lock-in techniques, for dispersion and detection purposes, respectively.

The compositions of the layers were determined using energy dispersive spectrophotometer attached to an ISI SS-40 scanning electron microscope. GaSb, GaP and InAs were used as the binary standards for Sb, Ga, In and As, respectively. The quantitative analysis

was carried out using Tracor Northern Computer. The MICROQ program with ZAF correction was used to analyze the x-ray spectra.

III RESULTS AND DISCUSSION

A. GROWTH RESULTS

GaSb and GaInAsSb layers of different compositions corresponding to the room temperature PL peak wavelength range of 1.7 to 2.32 μm were grown by the LPEE technique. $\text{Ga}_{1-x}\text{In}_x\text{As}_y\text{Sb}_{1-y}$ layers of compositions corresponding to room temperature PL peak wavelengths around 1.8 μm , 1.99 μm and 2.2 μm have been labelled as α , β and γ samples, respectively. The quaternary α and β layers were grown at 580°C, as better compositional homogeneity is expected due to the reduction in As distribution coefficient (7) at higher temperatures. However, for the growth of γ composition, catastrophic dissolution of the substrate occurred at this temperature due to the unstable melt. Hence the growth temperature was lowered to 530°C. The liquidus compositions of the different melts used were reported earlier (11). The growth parameters together with the results of lattice mismatch and the layer composition, where available, are given in Table 1. The growth rate exhibited a linear dependence with the current density (11), which is indicative of the dominance of the electrotransport mechanism in the growth process. The typical values of the growth rates as reported earlier (11) are 0.8 $\mu\text{m}/\text{min}$ at a current density of 10 A/cm². Layers in the thickness range of 1-10 μm have been grown by this technique. The layers used for the PL measurements were 2-4 μm thick.

X-ray diffraction studies of the grown layers indicated that epitaxial layer-GaSb substrate mismatch, $\Delta a/a$, never exceeded 0.17%. The full width half maxima (FWHM) of the epilayers

were in the range of 20-67 arcsec. The good quality of the crystalline epilayers becomes evident when this is compared to the half width of the 25-30 arcsec normally seen on the substrate itself. For α and β layers smooth and shiny surfaces were obtained with ease under both lattice matched and lattice mismatched conditions. This indicates that lattice matching is not critical for obtaining specular surfaces for compositions close to the GaSb corner of the phase diagram. For γ layers, the surface morphology was comparatively inferior, in general exhibiting cloudy appearance. However, the exact dependence of the surface morphology on the lattice mismatch was not examined in detail.

B. NEAR BAND EDGE PL SPECTRA AT 4.5K

Figure 2 illustrates the 4.5K PL spectra of LPEE grown GaSb and $\text{Ga}_{1-x}\text{In}_x\text{As}_y\text{Sb}_{1-y}$ epilayers. The PL emission intensity of the spectra has been normalized with respect to the dominant peak present in each of the samples. A quantitative fit to the PL spectra, using the sum of Gaussian line shapes, have been utilized to accurately determine the peak positions and the spectral widths.

As shown in Fig.2, in GaSb (sample GS-8) we observe four emission peaks labeled as BE_1 , BE_2 , BE_3 , and BE_4 at 805.4, 802.2, 799.1 and 795.8 meV, respectively near the band edge. These peaks have been associated with the radiative decay of excitons bound to neutral acceptors. The origin of these acceptors is not definitely known though some have been conjectured as due to native defects. In addition, a weak transition associated with free excitons (FE) is also observed at 808.5 meV which attests to the high quality of the LPEE grown layers. Amongst the bound exciton transitions, BE_2 is found to be the strongest and BE_1 appears to be

hidden by the more pronounced emission peak BE_2 . BE_3 and BE_4 also appear to be fairly strong.

The band - acceptor or donor - acceptor transition (A) at 777.5 meV is the dominant peak. In GaSb the donor levels are shallow (~ 2 -3 meV) due to the small effective mass of the electron, which makes it difficult to distinguish between free to bound and donor-to acceptor recombination processes. A broad band at the lower energy can be resolved to consist of impurity related transitions (B) and phonon replica of A (A-LO). In addition to most of the peaks reported in literature in LPE grown GaSb, an additional unidentified peak UI at 784.6 meV observed in MBE(35) and OMVPE (36) grown layers, is also seen.

The PL spectra of the quaternary layers exhibit features similar to those described for GaSb. PL spectral characteristics of the quaternary layers are summarized in Table 2. Free exciton transition is seen only in α -23 sample, as a weak band centered at 765.0 meV on the high energy side of the spectrum. This is seen in both GaSb and α -23 layers only under the highest excitation level used. The highest energy transition line identified as BE_2' at 760.5 meV becomes strong. In addition, we observe transitions at 754.3, 742.2, 730.6 and 702.2 meV which are labeled as BE_3' , UI, A, and A-LO, respectively. The transitions BE_2' and BE_3' are relatively sharp and are only 4.5 and 10.7 meV lower in energy than the free exciton line. We suggest that these two transitions are associated with the decay of excitons bound to two different neutral acceptors whose identity is not known at this time. As in GaSb the transitions A and A-LO are associated with the band-acceptor recombination and its optical phonon replica, respectively and transition A is the most intense. The energy band gap of this sample is obtained by adding the free exciton binding energy (~ 1.1 meV) to the free exciton transition energy (765.0 meV).

In sample β -9, which has an alloy composition corresponding to a lower band gap, we observe at least five transitions at 703.8, 697.9, 691.1, 670.9 and 640.2 meV labeled as BE_1' , BE_2' , BE_3' , A and A-LO, respectively. We do not see any evidence of the free exciton transition for the range of pumping power studied in this work, and therefore cannot accurately determine the value of the energy band gap in this sample. We find that the linewidths of BE_1' , BE_2' , and BE_3' transitions observed in this sample are comparable to those of acceptor bound excitons in GaSb and α -23 sample. We therefore suggest, as before, that these transitions are associated with the radiative decay of excitons bound to neutral acceptors. Additional support for this assignment is also provided by the excitation and temperature dependent behavior of these transitions as described in the later part of this paper. Thus if we assume that BE_1' is an acceptor bound exciton transition, we can estimate the band gap of this sample by adding approximately 4 meV (namely, the sum of the exciton dissociation energy and FE binding energy) to the transition energy of BE_1' namely 703.8 meV. This gives us a band gap of about 708 meV. The transition A, associated with the radiative recombination of a free electron with a bound hole of an acceptor is rather weak in this sample whereas in GaSb and in α -23, it is the most intense transition. It is not clear why this transition is so weak whereas an acceptor bound exciton transition BE_1' is so strong. From the value of the band gap and the transition energy of A we determine the binding energy of the acceptor to be 38 meV. This value compares quite well with those determined in GaSb (34 meV) and α -23 sample (35 meV).

A broad line shifted by ~ 30 meV from the A peak towards lower energy appears, as in the other two samples. We label this structure as LO phonon replica of A (A-LO), as this energy corresponds to the optical phonon energy reported in GaSb (37). In GaSb, α -23 and β -9 samples,

the ratios of the intensity of the A peak and A-LO peak are in the range 32-40 and remain invariant within experimental error with excitation laser power intensity and decrease with increase in temperature. This trend conforms to the expected behavior of the phonon sideband further strengthening the assignment of this peak. However, $\text{Ga}_{1-x}\text{In}_x\text{As}_y\text{Sb}_{1-y}$ alloy have an unusual band structure and the peak designated as A-LO could be related to it. Even though this transition is proposed to be a phonon replica of A, this identification is by no means definite.

In sample γ -11, which has an alloy composition corresponding to even a lower band gap, we observe three transitions at 607.1, 594.1 and 578.1 meV labeled as BE_1' , BE_3' and A, respectively. Again, we do not see a free excitonic transition. As in the case of sample β -9, we associate BE_1' and BE_3' with radiative recombination of excitons bound to two different neutral acceptors and estimate the band gap of this sample by adding about 4 meV to the transition energy of BE_1' , namely 607.1 meV. This leads to a band gap of about 611 meV. The transition A is very weak and could be detected only under high sensitivity. As before, we suggest that this transition is associated with radiative recombination of a free electron with a bound hole. The binding energy of an acceptor obtained in this case is about 33 meV which compares rather well with values obtained in GaSb and other two alloy samples. It should be pointed out that our observation of a single strong peak in γ -samples is consistent with the experimental observation (38) on the layers grown by non equilibrium techniques (OMVPE and MBE) where only one strong peak is seen for layers with compositions closer to or inside the miscibility gap region.

C. INTENSITY DEPENDENCE OF THE PL SPECTRA

To further confirm the identity of the various peaks, the PL spectra were studied as a

function of incident laser power intensity. The integrated intensity of BE_2' transition as a function of incident intensity for α samples is depicted in Figure 3. It exhibits a power dependence of $P^{1.40}$. The transitions identified as BE_3' in all the quaternary layers exhibit an identical power dependence of $P^{1.22}$, though only the intensity dependence of BE_3' in α samples is shown, suggesting that the BE_3' transitions in the different quaternary layers have similar origin. These values are somewhat higher than the power dependence of $P^{0.9}$ and $P^{1.14}$, respectively reported in GaSb layers for similar transitions by Chidley et al. (36).

In Fig.4 we display the variation of the integrated intensity of BE_1' transition in β -9 sample as a function of the incident power. This transition exhibits a power dependence of 2.1. Similar power dependence for this transition is also found in the other quaternary alloy γ -11. We have calculated the power dependence of the integrated intensity of transitions associated with the radiative recombination of excitons bound to neutral acceptors using the well known rate equations. We find that this dependence varies from $P^{1.0}$ to $P^{2.0}$ depending upon the values of the various recombination parameters which are highly sample dependent. Thus our assignment of BE_1' , BE_2' , and BE_3' transitions in $Ga_{1-x}In_xAs_ySb_{1-y}$ alloys to acceptor bound excitons is consistent with their behavior as a function of incident power.

With the decrease of incident laser intensity, the higher energy transitions gradually collapse and only the free electron to acceptor transitions persist at low intensities. The variation of the luminescence intensity of the free electron to acceptor peak in β -9 layer at 670.9 meV as a function of incident intensity is also shown in Figure 4. The intensity variation is perfectly linear with a slope of 1.0 confirming the assignment of this peak. No saturation effects in any of the peaks were observed in the limited range of incident laser power used.

D. TEMPERATURE DEPENDENCE OF THE PL INTENSITY

With increase in temperature, the overall integrated emission intensity of the quaternary PL spectra gradually decreases, indicating the presence of non-radiative mechanisms of decay with low activation energies. BE_2' in α layers shifts to higher energy by 0.57 meV with increasing temperature up to 30K, and thereafter merges with the band-to-band transitions. The deeper bound exciton peak identified as BE_3' is rapidly quenched by 35-40K with no significant shift in the position.

To determine the activation energies of the bound excitons, the low temperature integrated intensity dependent data for BE_3' were fitted as shown in Figure 5, using the three level Boltzmann distribution developed by Bimberg et al.(39)

$$I_T/I_0 = 1 / \{1 + C_1 \exp(-\Delta E_1/kT) + C_2 \exp(-\Delta E_2/kT)\}, \quad (1)$$

where I_T/I_0 represents the normalized integrated intensity at 4.5K, ΔE_1 and ΔE_2 represent the effective mass donor binding energy and dissociation energy of the bound exciton, respectively, C_1 and C_2 are constants and are functions of the density of states. The values of ΔE_1 and ΔE_2 were found to be in the range 1.1-1.3 meV and 8.9- 11 meV, respectively, in excellent agreement with the corresponding values reported in GaSb layers (33). The binding energy of the second level (4/3 of the thermal activation energy) is in the range of 11.8-14.6 meV, which is also close to the values estimated from the PL peak positions. The intensity of BE_1' transitions as a function of temperature could not be fitted with a reasonable set of values for ΔE_1 and ΔE_2 . The reason for this behavior is not clear at this time.

Integrated intensity of the band to acceptor transition also decreases with increase in temperature. However, it persists up to a temperature of 100-140K. In α layers the A peak

shifts to higher energy by 0.43 meV with rise in temperature up to 35K before it follows the band gap variation. This may be caused by the shift in the quasi Fermi level to higher values in the conduction band, and consequent recombination of the free electrons above the Fermi level with the holes localized in the acceptor states.

The band to band transitions are the only recombination processes above 80K in all the quaternary layers. With rise in temperature the integrated intensity of the band-to-band transition decreases. The activation energy for this thermal quenching process has been determined using the configuration coordinate model, where the competing nonradiative recombination process can be described by the expression

$$I = I_0 \exp(E_a/kT) \quad (2)$$

where I and E_a represent the PL emission intensity and quenching activation energy, respectively. The semilog plot of intensity versus reciprocal temperature is linear as illustrated in Fig. 6 exhibiting an activation energy of 14 meV in α layer and 28 meV in β and γ layers. The fact that these energies do not correspond to the band gap energy is indicative of the presence of various nonradiative centers in the quaternary layers. Such nonradiative recombination processes would degrade the performance of devices which have these alloys as active layers. They lead to a low value of T_0 for instance, which represents a characteristic temperature that relates to the laser threshold current density, J_{th} in the laser diode. The temperature dependence of J_{th} is described by

$$J_{th} = J_0 \exp(T/T_0) \quad (3)$$

where J_0 is the threshold current density at $T=0K$. Phenomenologically, temperature dependence of the PL process could be expressed in terms of T_0 as

$$I \propto \exp(-T/T_0) \quad (4)$$

The straight line fit of the integrated intensity with temperature as shown in Figure 7 yields the value of T_0 to be 225 K for α sample and ~ 90 K for β and γ samples, respectively. The latter result is in good agreement with the reported value of 80K in GaInAsSb/AlGaAsSb cw lasers (40); the emission wavelength at 190K being 2.1 μm , close to that of γ sample.

E. LINE SHAPE ANALYSIS

For GaSb and quaternary samples all the PL peaks could be well fitted by sum of the Gaussian line distributions at low temperatures. With rise in temperature the PL spectra become increasingly asymmetrical, and the asymmetry sets in around 25-35K range indicating the dominance of the band to band transitions. The PL spectral shape of band to band transition is analyzed (41) using

$$I(\omega) \propto (\hbar\omega - E_g)^{1/2} \exp[-(\hbar\omega - E_g)/kT], \text{ for } \hbar\omega > E_m \quad (5)$$

$$\propto \exp[(\hbar\omega - E_g)/\epsilon], \text{ for } \hbar\omega < E_m \quad (6)$$

where ϵ is the tail state parameter and E_m is the PL peak energy. The slope of the high energy side of the spectrum is dependent on the sample temperature, while the lower energy side of the spectrum is determined by the shape of the band edges. Figure 8 shows the experimental spectra and analytical fit for γ layer at 80 K. Similar fit has been obtained for all the quaternary layers in the temperature range of 30-300K with ϵ ranging from 3-10 meV. A similar behavior has also been observed in another quaternary GaInAsP/InP system (42). This suggests that localized states formed either due to impurities or compositional grading contribute to the recombination processes. At higher temperatures, the emission spectra are narrower than

the analytical spectra on the high energy side, as self absorption due to higher photon energy within the epilayer has not been taken into account. The value of E_g determined from this analysis was found to be $kT/2$ less than the PL peak energy indicative of k-conservation nature of the recombination processes.

The value of FWHM of the bound excitons for the quaternary alloys were in the range of 4-7meV at 4K. These are the smallest linewidths reported for $Ga_{1-x}In_xAs_ySb_{1-y}$ on GaSb so far. Variation of the FWHM of the band-to-band transitions the layers with temperature was also examined. Though there is a considerable scatter in the data, the experimental values for FWHM appear to increase linearly with temperature for all the layers, as shown in Figure 9. The slopes of the lines are 1.0k, 0.8k and 1.2k for all the three layers α , β , and γ , respectively and are much smaller than the analytical value of 1.8-2 k for intrinsic band to band transition computed from Eq.(5). Similar discrepancy between the experimental and the computed half width dependence on temperature has also been noticed in $Ga_{1-x}In_xAs_yP_{1-y}$ system (43,44) and, as mentioned earlier, is commonly attributed to the overestimation of the spectral width by van Roosbroeck Shockley relation (Eq.5). However, the narrow linewidths observed in our quaternary samples indicate high quality of the crystalline layers.

And finally, we would like to point out that our proposed assignment of the near band edge emission peaks, BE_1' , BE_2' , and BE_3' to radiative recombination of excitons bound to different neutral acceptors in $Ga_{1-x}In_xAs_ySb_{1-y}$ layers is based on their relatively narrow widths and their behavior as a function incident laser power and temperature. However, there are a few aspects of our data which are rather intriguing. For instance, in sample α -23, both the bound exciton peak BE_2' , and electron-to-acceptor transition A are quite strong. However, in samples β -9 and

γ -11, the intensities of peaks A are much smaller than those of BE_1' . If BE_1' transition is due to exciton bound to neutral acceptors, as we have suggested, then the electron to the same acceptor transition should have been quite strong. Also in GaSb and sample α -23, we see several bound exciton peaks, but only one strong electron-to-acceptor transition. It is clear that more work needs to be done, especially in higher purity samples, to understand these features and to gain a better understanding of the nature of the acceptors.

III CONCLUSIONS

Good optical device quality layers of GaSb and $Ga_{1-x}In_xAs_ySb_{1-y}$ have been grown by LPEE technique as evidenced by the narrow spectral width of x-ray diffraction and PL spectra. A systematic trend in the low temperature PL spectra is observed with the change in the composition of $Ga_{1-x}In_xAs_ySb_{1-y}$. The optical activation energy of the acceptor is about 35 meV and its phonon replica is shifted by about 30 meV towards the lower energy, consistent with the reported values in GaSb. The dissociation energies of the bound excitons in quaternary layers were also in good agreement with those in the binary layers. A good fit to the PL spectral line shape due to band-to-band transition was obtained using the simple model of van Roosbroeck-Shockley at higher energies and exponential band edge at lower energies. The PL transitions appear to be k-conserved from the data presented.

ACKNOWLEDGEMENTS

We wish to acknowledge Lori Small for assisting in the computer simulation of a few of the graphs, Soon Lau from AT&T Bell Labs and Mike Caparo for x-ray diffraction measurements and Gernot Pomrenke for helpful suggestions. This work was supported by AFOSR (Contract # F49620-89-C-004) and USARO (Grant # DAAL03-89-G-0115). Work of

S.H. was supported by Air Force (Contract # F33615-88-C-5423)

Table I Summary of growth conditions and characterization results

Sample No.	Growth Temp. (°C)	Current Density (A/cm ²)	Thickness (μm)	λ_{μ} (μm)	E _g (eV)	ΔE _g meV	Δa/a %	FWHM (arc-sec)	x	y
GS#5	580	1.4	6.5	1.70	.729	32				
GS#8				1.70	.729	43			0.00	0.00
GS#29				1.71	.729	37	.00	24	0.00	0.00
G3α3				1.77	.700	41		30		
αT-05	580	6.2		1.79	.693	42	.00	67		
αT-11	581	6.0		1.79	.693	35	.01	32	.027	.014
αT-02	580	8.2		1.81	.685	37	-.07	27		
α-23	581	10.4		1.81	.685	39	.00	31	.028	.016
αT-14	581	6.5		1.82	.681	44	.04	30		
α-21	581	9.9	5.5	1.84	.674	35	.04	20		
β-8				1.95	.636	28				
β-9				1.96	.633	32	.048*		.088	.056
β-120	574			1.96	.633	35	.001	30	.098	.058
βT-22	585	9.8	7.3	1.97	.629	37	<.050*	42		
βT-27	572	7.5	3.7	1.99	.623	35	-.042	27	.066	.078
β-121	574			1.99	.623	23	-.083	40		
β-18	573	6.8	5.4	2.00	.620	33	.06	46		
γ-11	534	11.4	2.9	2.25	.551		.00*	55		
γT-31	535	11.3	0.7	2.25	.551	48	.00	22	.170	.140
γT-47	532	18.7	3.7	2.26	.549	37	-.164*	61	.173	.157
γT-46	535	14.4	4.0	2.27	.546	37	-.099*	28	.199	.160
γT-44	535	8.9	3.7	2.27	.546	45	.083*	66	.191	.164
γ-12	534	11.8	6.6	2.28	.544	37	.079*	65	.208	.165
γ-14	533	11.7	3.7	2.30	.539	41				
δAF-7	529	10.0	5.6	2.32	.534	46			.195	.154

*Indicates that the lattice mismatch was determined by high resolution x-ray diffraction.

TABLE II Low temperature PL characteristics of LPEE grown GaInAsSb layers.

α -23				β -9			γ -11		
Iden	Energy (mev)	FWHM	Rel. Int.	Energy (mev)	FWHM	Rel. Int.	Energy (mev)	FWHM	Rel. Int.
FE	765.0	4.7	0.11						
BE ₁ '				703.8	5.0	1.0	607.1	5.5	1.0
BE ₂ '	760.5	4.1	1.00	697.9	5.2	0.04			
BE ₃ '	754.3	7.6	0.48	691.1	6.7	0.07	594.1	7.6	0.02
UI	742.2	14.0	0.07						
A	730.6	8.5	0.97	670.9	15.7	0.08	578.1		0.002
A-LO	702.2	8.8	0.03	640.2					

FIGURE CAPTIONS

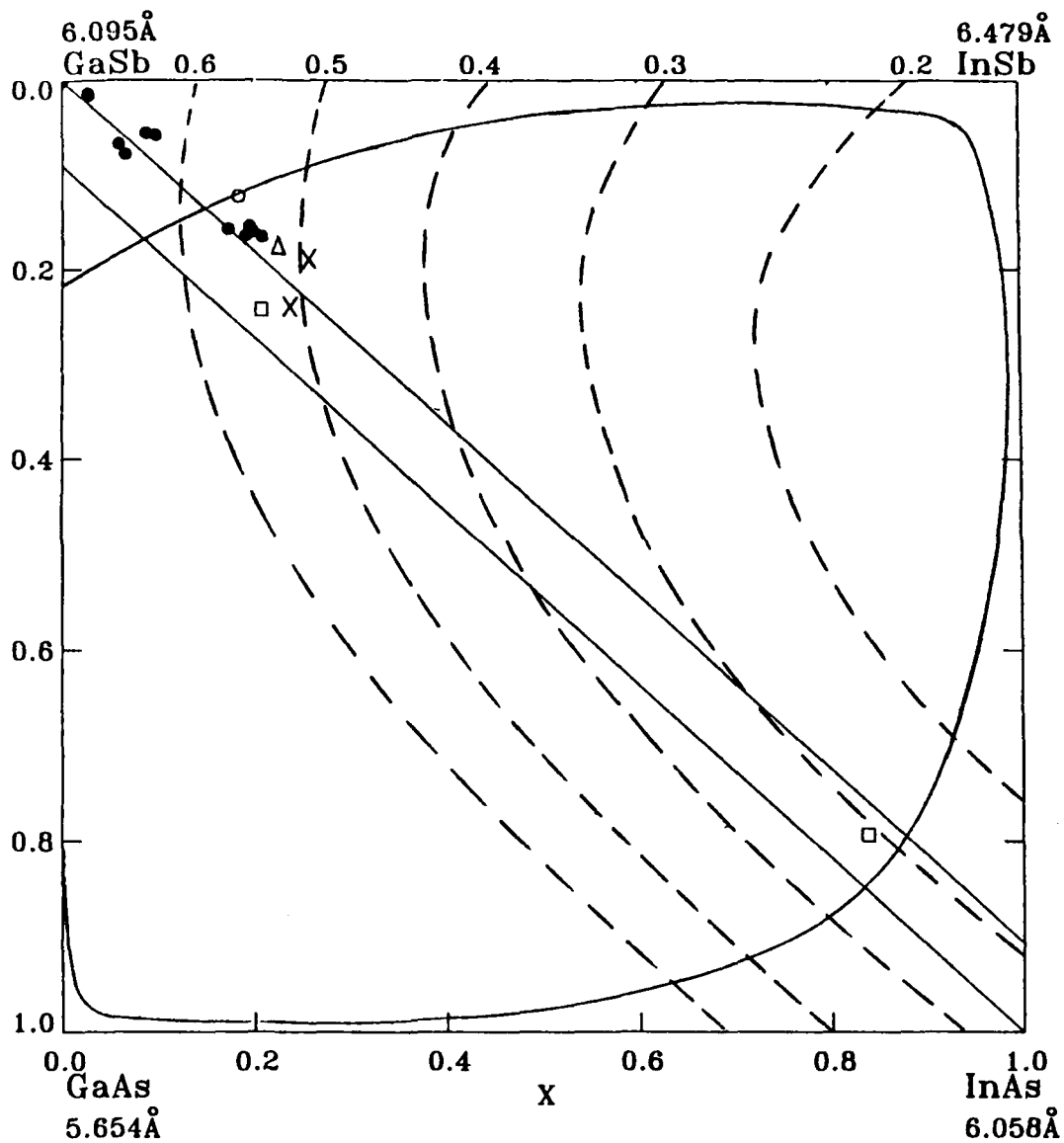
1. Schematic diagram of the solid phase field for the quaternary alloy system Ga-In-As-Sb. Isolattice constant lines for alloys lattice matched to GaSb and InAs are shown by the solid straight lines. Binodal isotherm at 600°C and room temperature band gap plots are taken from ref (1). Indicated are our data points (o), previous LPE data corresponding to the highest value of x inside the gap -(a) lattice matched to GaSb, DeWinter et al.(5)(Δ), Jouille et al.(6)(x) -(b) lattice matched to InAs, Sankaran et al.(8) (\square) and Astles et al.(7)(\circ).
2. Low temperature (4.5K) PL spectra of GaSb and GaInAsSb of three different compositions.
3. Variation of PL integrated intensity of the bound excitons as a function of the incident laser intensity in α layers.
4. PL integrated intensity dependence of band to band transitions and band to acceptor transitions in β layers on the incident laser intensity.
5. Theoretical fit to the temperature dependence of integrated intensity of deeper bound exciton transition (BE_3') at low temperatures. The values of C_1, C_2 , and the binding energies are in excellent agreement with the results of GaSb (33).
6. Thermal quenching behavior of band to band PL emission for temperatures beyond 80K. The intensity of the γ layers were scaled up so that they can be plotted on the same graph.
7. Semilog plot of integrated intensity of band-to-band transitions as a function of temperature for all three different compositions of GaInAsSb.
8. Analytical fit to the PL spectra of γ layers at 80K. The band tail state parameter $\epsilon=3$ meV was used to get the best fit to the lower energy side of the spectrum.
9. Temperature dependence of the FWHM of band-to-band transitions in GaInAsSb layers.

REFERENCES

1. M.J. Cherng, H.R. Jen, C.A. Larsen, G.B. Stringfellow, H. Lundt and P.C. Taylor, J. Cryst. Growth **77**, 408 (1986).
2. M.J. Cherng, G.B. Stringfellow, D.W. Kisker, A.K. Srivastava and J. L. Zyskind, Appl. Phys. Lett. **48**, 419 (1986).
3. T.H. Chiu, J.L. Zyskind and W.T. Tsang, J. Electron. Mat. **16**, 57(1987).
4. W.T. Tsang, T.H. Chiu, D.W. Kisker and J.A. Ditzenberger, Appl. Phys. Lett. **46**, 283 (1985).
5. J.C. DeWinter, M.A. Pollack, A.K. Srivastava and J.L. Zyskind, J. Electron.Mat.**14**, 729 (1985).
6. A. Joullie, F. Jia Hua, F. Karouta and H. Mani, J. Cryst. Growth **75**, 309 (1986).
7. M. Astles, H.Hill, A.J. Williams, P.J. Wright and M.L. Young, J. Electron. Material **15**, 41 (1986).
8. R.Sankaran and G.A.Antypas, J. Cryst. Growth **36**,198 (1976).
9. E. R.Gertner, A.M. Andrews, L.O. Bubulac, D.T. Cheung, M. J. Ludowise and R. A. Riedel, J. Electron. Mater. **8**, 545 (1979).
10. N. Kobayashi and Y. Horikoshi, Jpn. J. Appl. Phys. **20**, 2253 (1981).
11. Shanthi N. Iyer, Ali Abul-Fadl, Albert T. Macrander, Jonathan H. Lewis, Ward J. Collis and James W. Sulhoff, Mat. Res. Symp. Proc. **160**, 445 (1990).
Layer Strucyure: Heteroepitaxy, Superlattices, Strian and Metastability. Editors. B.W.Dodson, LK.Schowalter, J.E.Cunningham and F.H.Polk
12. A. Okamoto, J. Lagowski and H.C. Gatos, J. Appl. Phys. **53**, 1706 (1982).

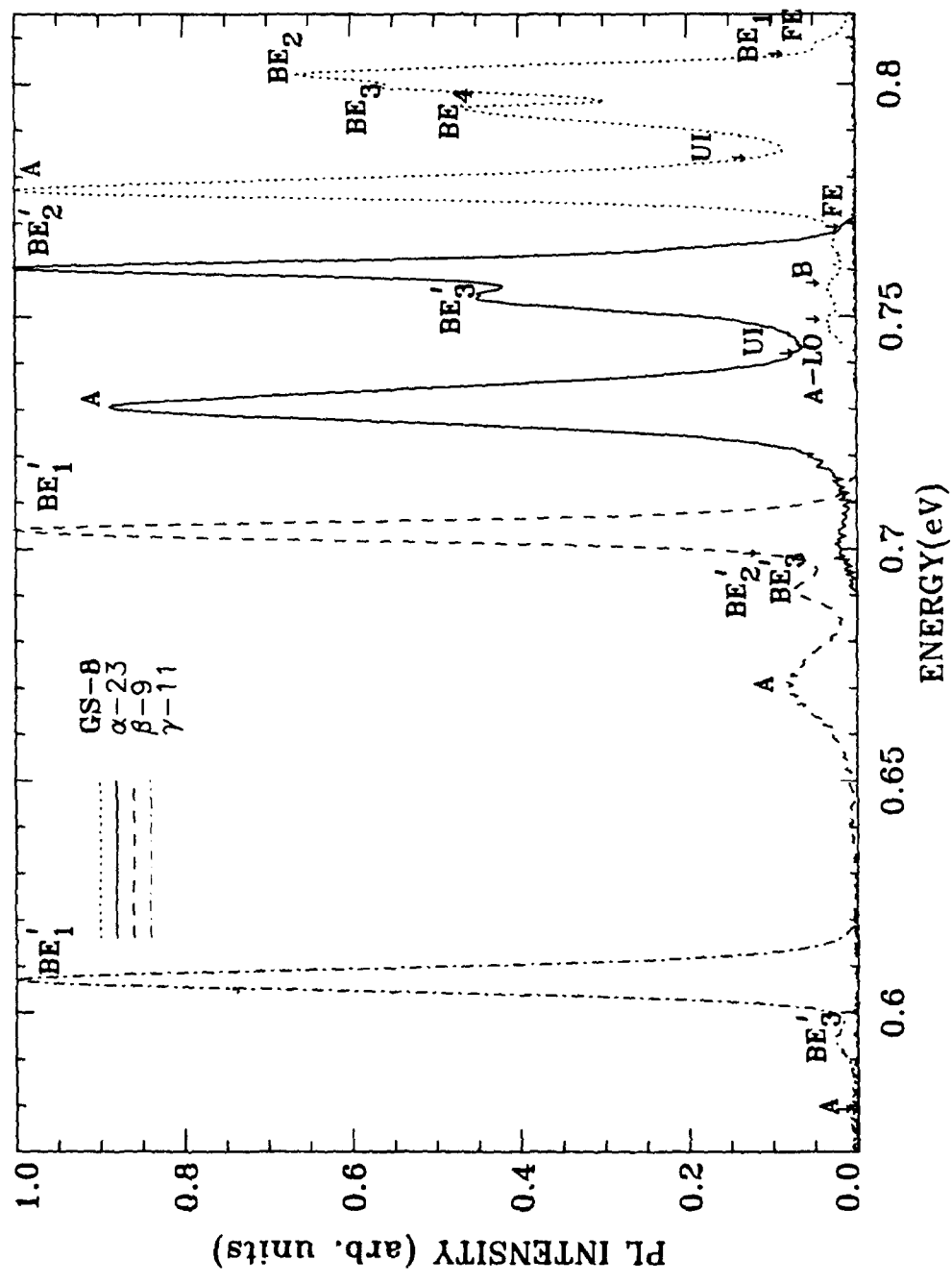
13. Y. Imamura, L. Jastrzebski and H.C. Gatos, *J. Electrochem. Soc.* **125**, 1560 (1978).
14. J.J. Daniele and A. Lewis, *J. Electron. Mater.* **12**, 1015 (1983).
15. J. J. Daniele and A. J. Hebling, *J. Appl. Phys.* **52**, 4325 (1981).
16. M. Kumagawa, A. F. Witt, M. Lichtensteiger, and H. C. Gatos, *J Electrochem. Soc.* **120**, 583, (1973).
17. C.Takenaka,T.Kusunoki and K.Nakajima, *J.Cryst.Growth* **114**,293(1991).
18. Toshiharu Kawabata and Susumu Koike, *Appl. Phys. Lett.* **43**,490 (1983).
19. S. Iyer, E.K. Stefanakos, A. Abul-Fadl and W. J. Collis, *J. Cryst. Growth* **67**,337 (1984).
20. A. Abul-Fadl, E.K. Stefanakos and W.J. Collis, *J. Electron. Mater.* **11**,559 (1982).
21. K. Nakajima and S. Yamazaki, *J. Cryst. Growth* **74**, 39 (1986).
22. S. Iyer, E.K. Stefanakos, A. Abul-Fadl and W.J.Collis, *J. Cryst. Growth* **70**,162 (1985).
23. D. Effer and P.J. Etter, *J. Phys. Chem. Solids* **25**, 451 (1964).
24. M.H. van Maaren, *J. Phys. Chem. Solids* **27**, 472 (1966).
25. Y.J. Van Der Meulen, *J. Phys. Chem. Solids* **28**, 25 (1967).
26. C. Anayama, T. Tanahashi, H. Kuwatsuka, S. Nishiyama, S. Isozumi and K. Nakajima, *Appl. Phys. Lett.* **56**, 239 (1990).
27. C. Benoit a la Guillaume and P. Lavallard, *Phys. Rev. B* **5**, 4900 (1972).
28. A.S. Kyuregyan, I.K. Lazareva, V.M. Stuchebnikov and A.E. Yunovich, *Tekhi. Poluprovodn.* **6**, 242 (1972) *Sov. Phys.-Sem.* **6**, 208 (1972).
29. A.A. Kastal'skii, T. Risbaev, I.M Fishman and Yu. G. Shreter, *Sov. Phys.-Sem.* **5**,1391, (1972).
30. E.J. Johnson and H. Y. Fan, *Phys. Rev.* **139**, A1991 (1965).

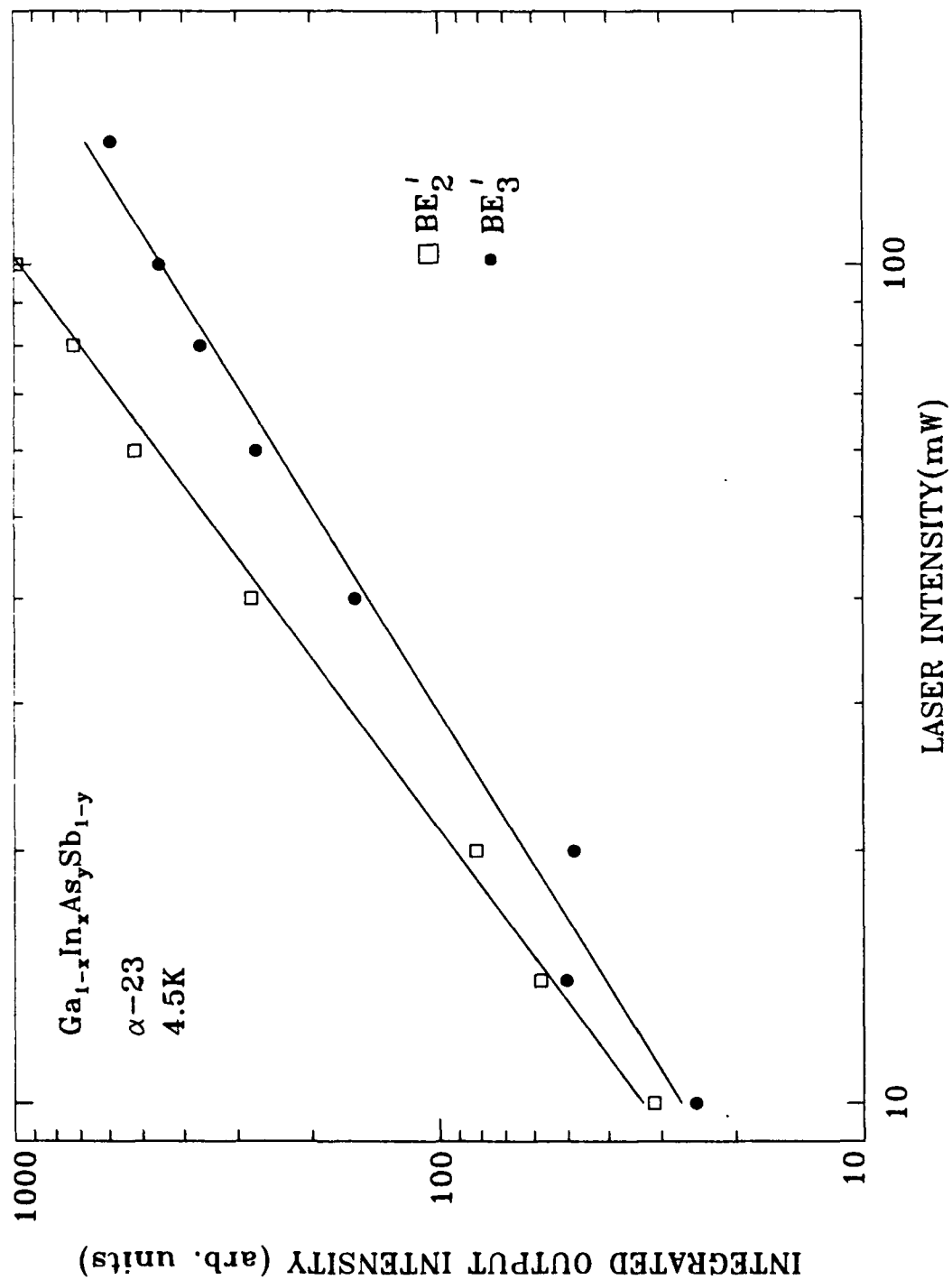
31. W. Jakowetz, W. Ruhle, K. Breuninger and M. Pilkuhn, Phys. Stat. Sol. (A) 12, 169 (1972).
32. W. Ruhle and D. Bimberg, Phys. Rev. B 12, 2382 (1975).
33. W. Ruhle, W. Jakowetz, C. Wolk, R. Linnebach and M. Pilkuhn, Phys. Stat. Sol. (B) 73, 255 (1976).
34. Fred H. Pollak and R.L. Aggarwal, Phys. Rev. B 4, 432 (1971).
35. M. Lee, D.J. Nicholas, K.E. Singer and B. Hamilton, J. Appl. Phys. 59, 2895 (1986).
36. E.T.R. Chidley, S.K. Haywood, A.B. Henriques, N.J. Mason, R.J. Nicholas, and P.J. Walker, Semicond. Sci. Technol. 6, 45 (1991).
37. C. Pickering, J. Electron. Mater. 15, 51 (1986).
38. S.J. Eglash and H.K. Choi, Gallium Arsenide and Related Compounds, 1991; Inst. Phys. Conf. Ser. No. 120 ed. G.B. Stringfellow (America Inst. of Physics, 1992) p.487
39. D. Bimberg, M. Sondergeld and E. Grobe, Phys. Rev. B 4, 3451 (1971).
40. C. Caneau, A.K. Srivastava, J.L. Zyskind, J.W. Sulhoff, A.G. Dentai and M.A. Pollack, Appl. Phys. Lett. 49, 55 (1986).
41. E.W. Williams and H.B. Bebb, in Semiconductors and Semimetals, Vol. 4, eds. R.K. Willardson and A.C. Beer, (Academic Press, 1972), Ch.4.
42. Ernst O. Gobel, in GaInAsP Alloy Semiconductors, ed. T.P. Pearsall (A Wiley Interscience Publication, 1982), p.320.
43. T.P. Pearsall, L. Eaves and J.C. Portal, J. Appl. Phys. 54, 1037 (1983).
44. H. Kyuragi, A. Suzuki, S. Matsumura and H. Matsunami, Appl. Phys. Lett. 37, 723 (1980).

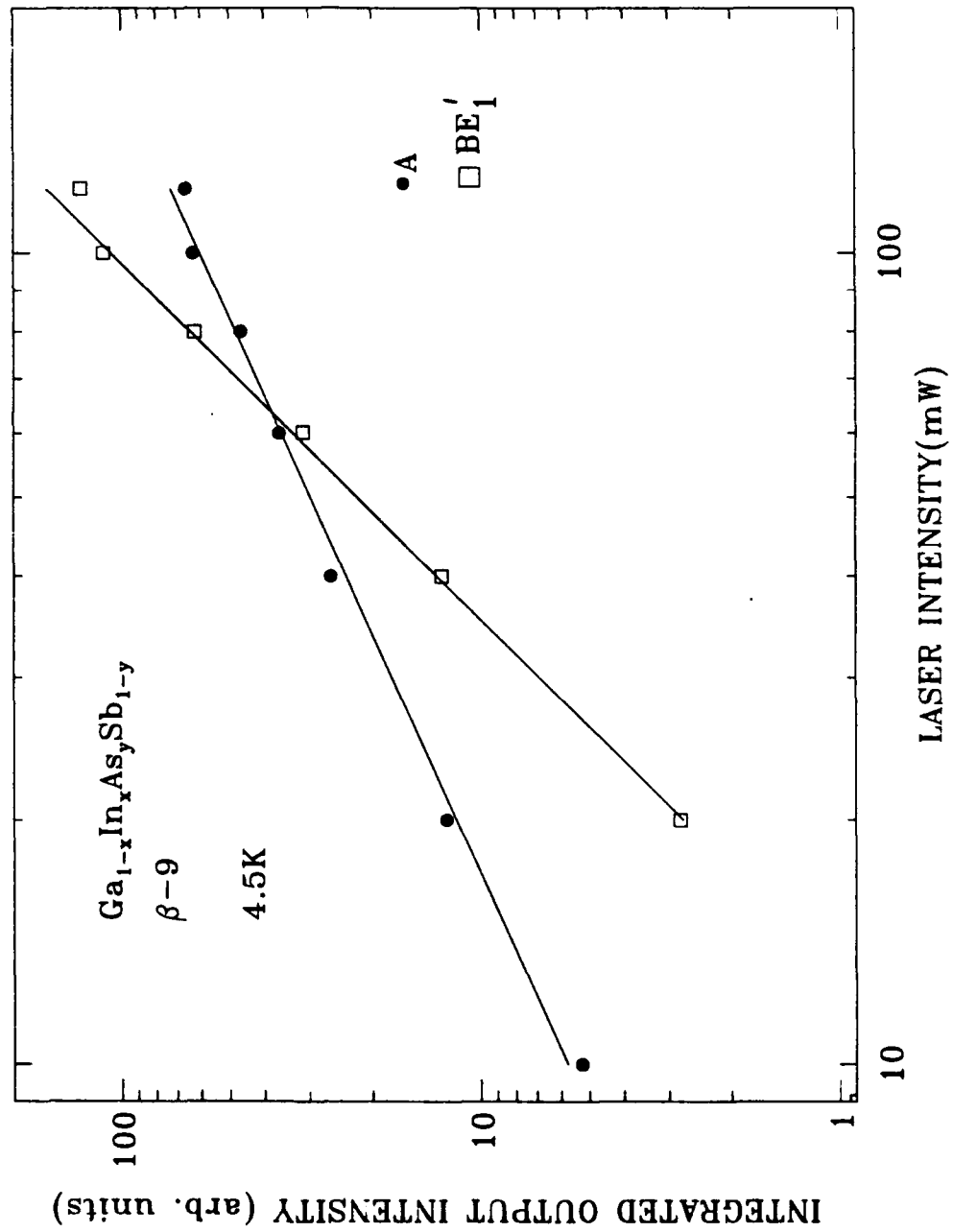


S. Iyer et al
Figure 1.

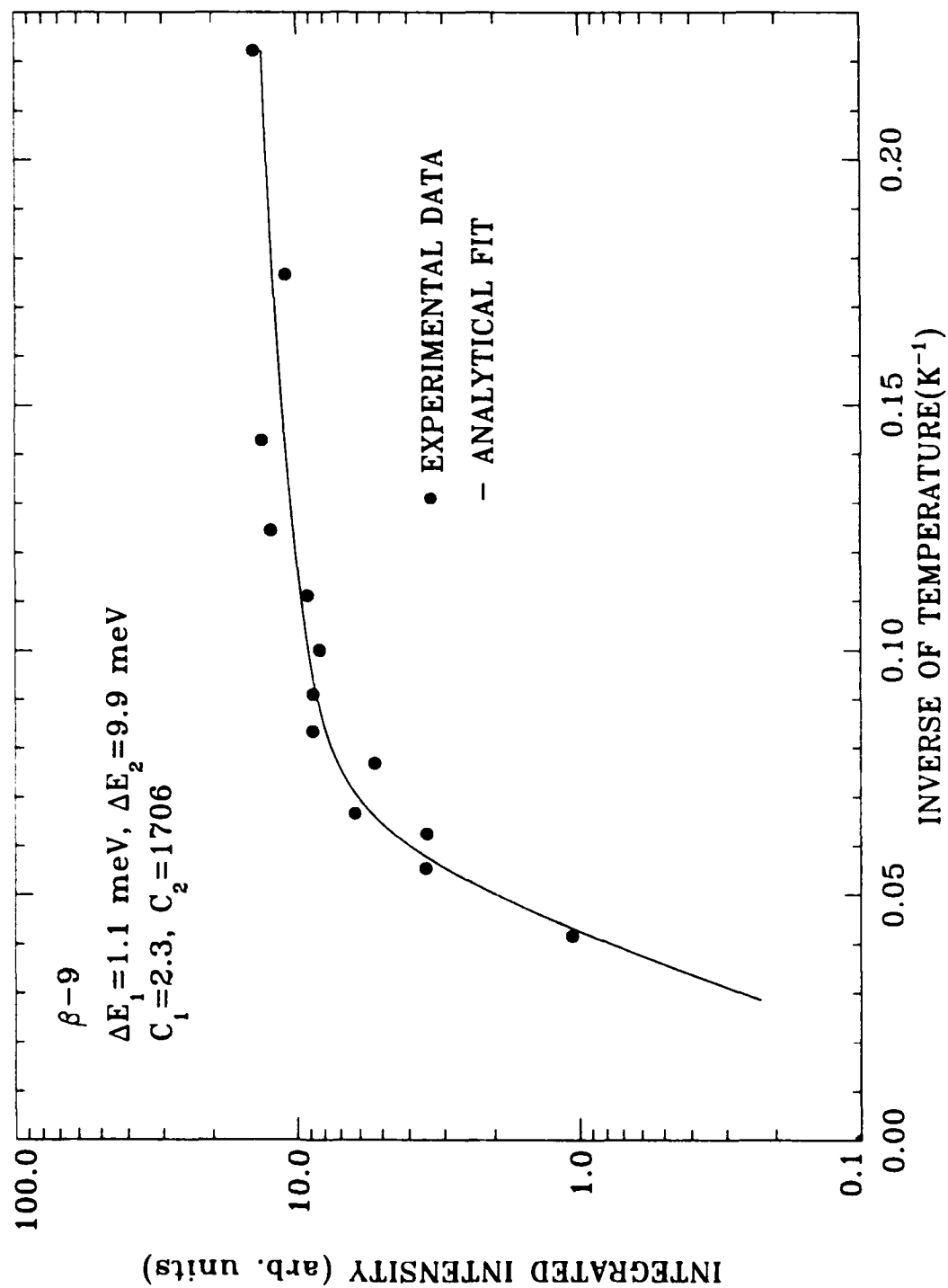
S. Iyer et al
Figure 9



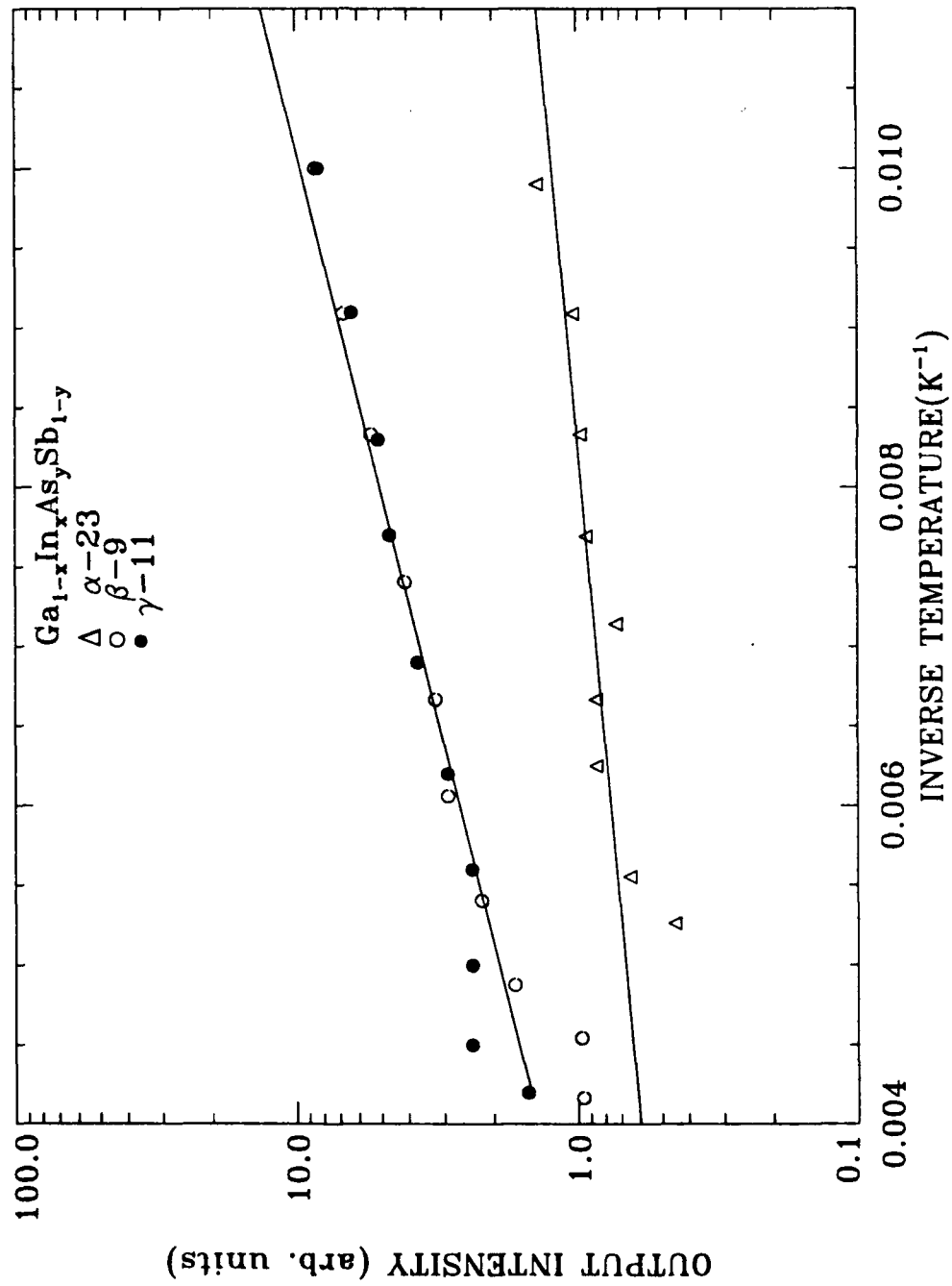




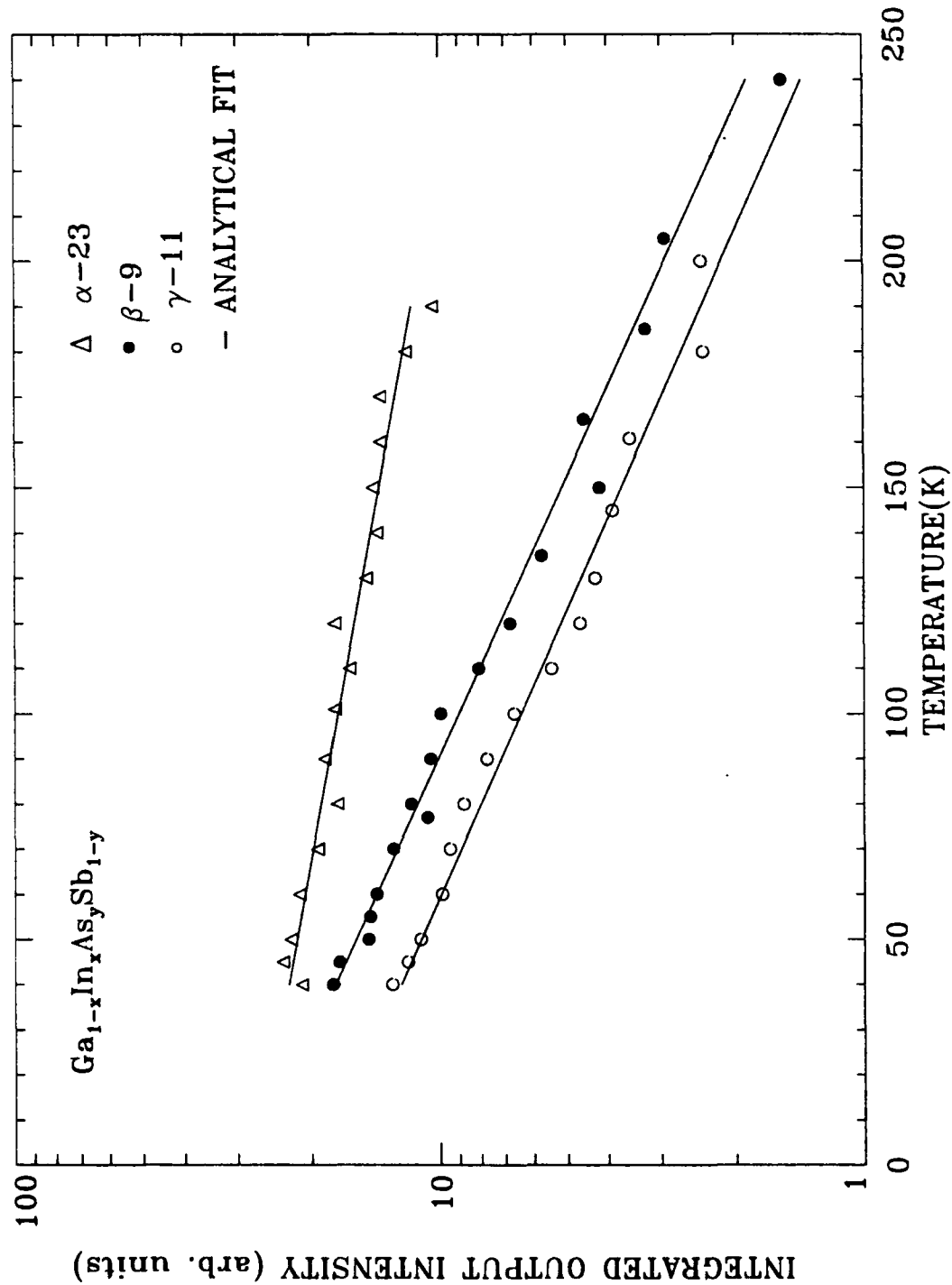
S Tyer et al.
Figure 4



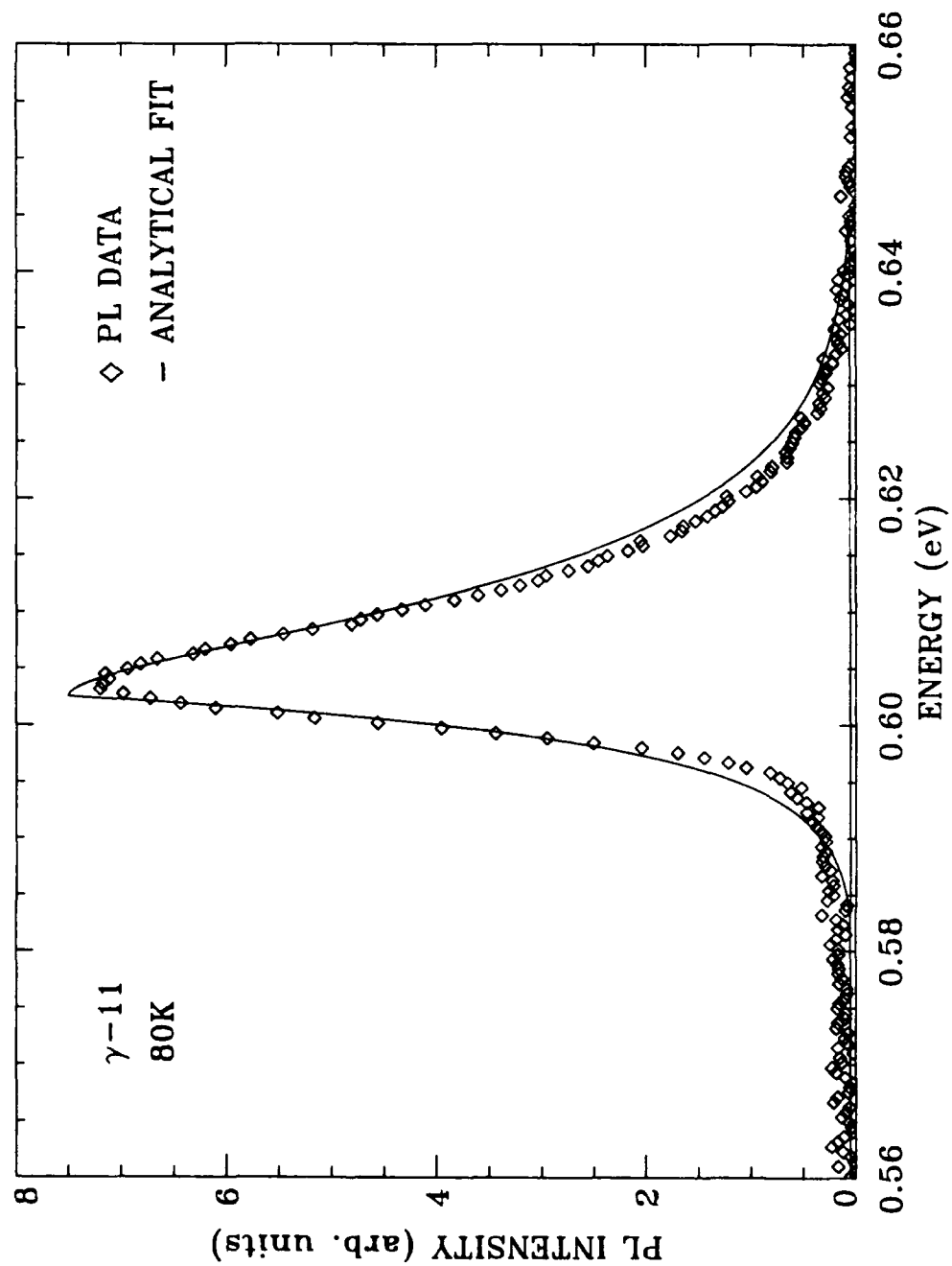
July 21, 2000



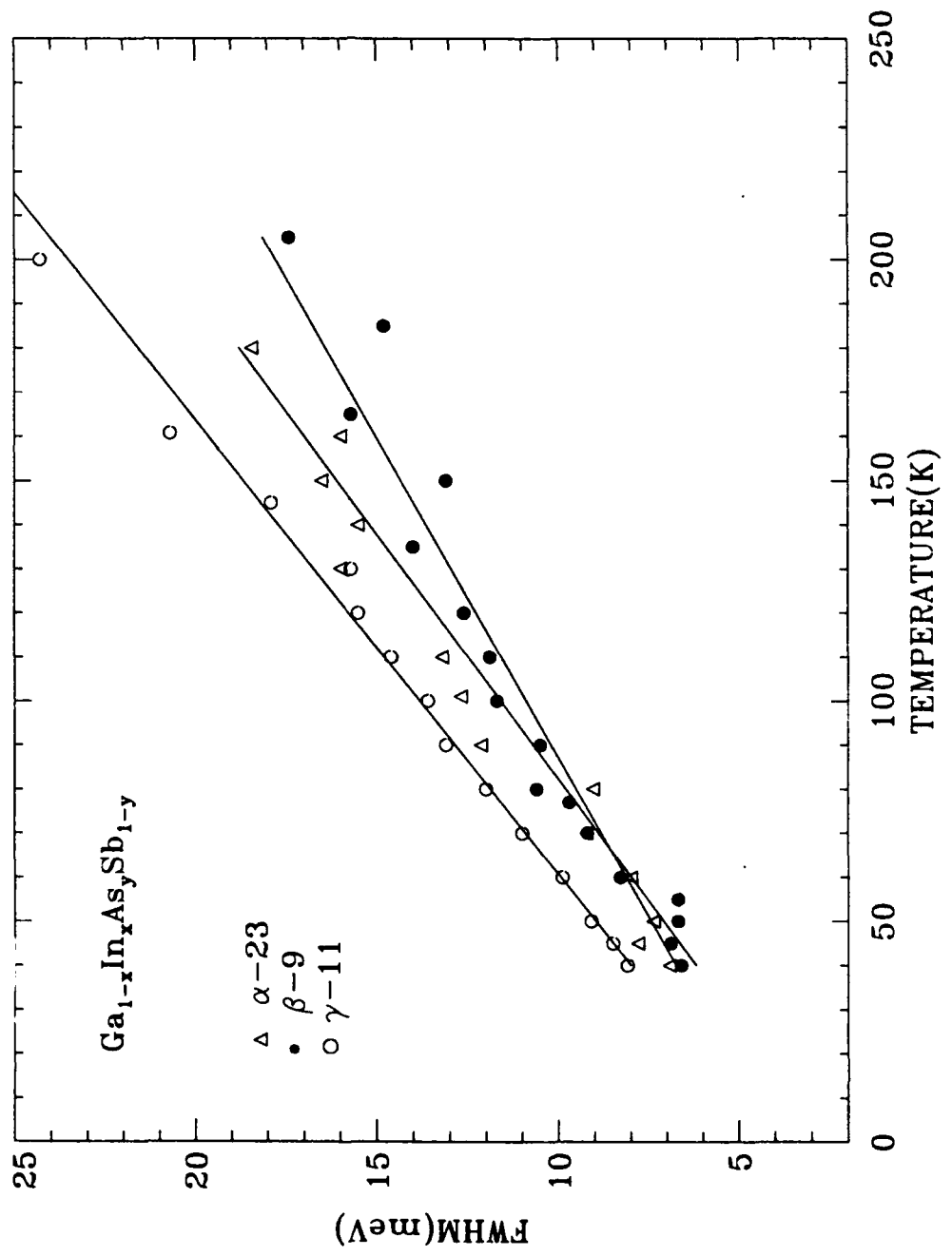
S. Iyer et al.
Figure 6



S. Iyer et al
Figure 7



S Iyer et al
1991



S. Iyer et al
Figure 9

APPENDIX C

**J. Appl. Phys. (to be pulished in
Mar.1993 issue)**

PHOTOLUMINESCENCE STUDY OF LIQUID PHASE ELECTROEPITAXIALLY GROWN GaInAsSb ON (100)GaSb

S. Iyer

Department of Electrical Engineering
North Carolina A&T State University
Greensboro, NC 27411

S. Hegde

University of Dayton Research Institute
Dayton, OH 45649-0178

K.K. Bajaj

Department of Physics, Emory University
Atlanta, GA 30322

Ali Abul-Fadl

Department of Electrical Engineering
North Carolina A&T State University
Greensboro, NC 27411

W. Mitchel

Materials Directorate, Wright Laboratory,
Wright Patterson Air Force Base, OH 45433-6533

ABSTRACT

Low temperature (4.5 K) photoluminescence (PL) spectra of liquid phase electroepitaxially (LPEE) grown GaSb and GaInAsSb have been examined. The excitonic transitions observed in GaSb and GaInAsSb layers of compositions close to the GaSb corner of the phase diagram, indicate an excellent quality of the grown layers. A systematic trend in the low temperature PL spectra is observed with the change in the alloy composition. The overall PL emission efficiency decreases and the number of excitonic transitions are fewer with the shift in the composition towards the lower band gap. Shift in the PL peak energy corresponding to the band to band transition with temperature was determined. The linear part of the shift above 100K, exhibits a slope of -0.3 meV/K .

PACS NOS. 78.55.Cr, 71.55.Eq, 71.35.+z, 81.15.Lm.

I INTRODUCTION

Low temperature photoluminescence (PL) has proven to be an effective method for characterization of GaSb system, in particular for the layers grown by near equilibrium techniques where the choice of the substrate is severely limited. PL studies of GaSb grown by LPE (1-3), MBE (4,5) and MOCVD (6) have been made by a number of workers. The presence of large background concentration of defects/impurities in this material lead to numerous acceptor bound exciton luminescence. Many of these transitions appear to be growth specific. Although there has been several reports on GaSb, there has been no detailed study reported to date on radiative transitions in GaInAsSb.

We have reported earlier (7) the first results on the growth of GaSb and GaInAsSb by Liquid Phase Electroepitaxial (LPEE) technique. This is a modified version of the LPE technique where an electric current passing through the substrate-solution interface enables better control of the growth rate (8), enhances the interface stability (9) leading to a better compositional homogeneity (10) in the epilayers and significant improvement in the surface morphology (11).

In this paper we report the low temperature (4.5K) Fourier transform photoluminescence (PL) study of the LPEE grown epilayers of GaSb and $\text{Ga}_{1-x}\text{In}_x\text{As}_y\text{Sb}_{1-y}$. Samples of GaSb and three different compositions of quaternary alloys $\text{Ga}_{0.028}\text{In}_{0.972}\text{As}_{0.016}\text{Sb}_{0.984}$, $\text{Ga}_{0.088}\text{In}_{0.912}\text{As}_{0.056}\text{Sb}_{0.944}$ and $\text{Ga}_{0.17}\text{In}_{0.83}\text{As}_{0.14}\text{Sb}_{0.86}$ labelled as α -23, β -9 and γ -11, respectively were studied. The layers α -23 and γ -11 were lattice matched to (100) GaSb substrate while β -9 was mismatched by 0.048%. The room temperature PL peak wavelengths of band edge related peaks in these samples ranged from 1.7 μm to 2.28 μm . The results of the variation in the PL spectral characteristics with composition and the temperature dependence of the band edge related transitions are reported.

II EXPERIMENTAL DETAILS

The details of the growth and characterization of the layers are described elsewhere (7). Layer compositions were determined using energy dispersive x-ray analysis. Photoluminescence spectra were obtained using a Bomem Fourier transform spectrometer and a cooled (77 K) InAs detector. The samples were immersed in a variable temperature continuous flow liquid helium cryostat and were excited with 514.5 nm line of an Ar-ion laser.

III RESULTS AND DISCUSSION

Figure 1 illustrates the PL spectra of LPEE grown GaSb and GaInAsSb epilayers. The PL emission intensity has been normalized with respect to the dominant peak present in each of the samples. Integrated intensity, exciton dissociation energy and assignment of the observed peaks in 4.2K PL energy spectra of GaSb and GaInAsSb samples are summarized in Tables 1 and 2, respectively. The energy position and full width at half maximum (FWHM) of each peak have been determined by a quantitative fit to the experimental PL spectra using sum of Gaussian line distributions.

As illustrated in Figure 1, in GaSb (GS-8) five band edge PL emission peaks labeled as FE, BE₁, BE₂, BE₃ and BE₄ are observed at 808.5, 805.4, 802.2, 799. and 795.8 meV, respectively as in the LPE grown layers. The presence of a weak broad shoulder at 808.5 meV has been associated with the free exciton (FE). This indicates the good quality of the crystalline LPEE layers. The other lines have been attributed to the decay of excitons bound to the neutral acceptors. BE₂ has been ascribed (12,13) to the decay of an exciton bound to a dominant residual acceptor level, which has a binding energy of 34 meV. Little is known

about the acceptors corresponding to the two transitions BE_1 and BE_3 , while there are conflicting reports (2, 13-15) as to the origin of the transition BE_4 . In the LPEE grown layers unlike LPE, BE_2 is found to be the strongest peak amongst the bound excitons. The band to acceptor transition (A) at 777.5 meV is found to be the dominant peak in the PL spectra and this acceptor with a binding energy of 34 meV has been associated with a complex native defects due to Sb vacancies (16,17). In addition to these a broad band at a lower energy can be resolved to consist of acceptor related transition (B) with a binding energy of 54 meV, phonon replica of A and an unidentified line at 784.8 meV. This unidentified line has also been reported in MBE(4) and MOCVD (6) grown layers. The bound excitons are somewhat broader (with FWHM 1-5 meV) than in the best LPE grown layers with FWHM as low as 0.3 meV for BE_1 reported in the literature (1). However, it is to be noted that no extensive baking of the melt was carried out prior to the growth of these layers as our primary objective was to use the PL spectral features of GaSb as a reference to get a better understanding of the transitions in the alloy system.

The PL spectra of the quaternary layers exhibit features similar to those described for GaSb layers, however a fewer near band edge structures are seen in general. A definite trend in the overall PL spectra is seen with the shift in the composition towards InAs. The overall integrated intensity remains the same for GaSb, α and β layers, but decreases by almost a factor of five to ten for γ samples. Free exciton (FE) transition is seen only in α -23 sample as a weak band on the higher energy spectrum. This feature is seen in both GaSb and quaternary layers under the highest excitation level used, typical of free exciton. In addition, two sharp band edge related transitions (labeled as BE_2' and BE_3') with FWHM of 4 meV and 7 meV,

respectively are observed. With the shift in the composition towards higher values of x , the highest energy transition line identified as BE_1' becomes dominant accompanied with a weaker transition BE_3' shifted by 12-13 meV towards the lower energy side. We suggest that these transitions labelled as BE' are associated with the decay of excitons bound to different neutral acceptors with different concentrations leading to different PL intensities. Our assignment is primarily based on the values of their line widths and the observed temperature and excitation intensity dependence. Firstly, the spectral distribution of the bound excitons is found to be close to Gaussian with a relatively narrow FWHM in the range of 3-7 meV. Secondly, the variation of the PL integrated intensity with the excitation intensity revealed a slope of 2 for BE_1' in β and γ layers, 1.4 for BE_2' in α layers and 1.22 for BE_3' in α and β layers (18). We have computed the value of this slope using the well known rate equations. It is found that this value may vary from 1 to 2 depending upon the values used for various recombination parameters which are highly sample dependent. Thirdly, these transitions are rapidly quenched with increasing temperature by 35-40K. All these observations are consistent with the expected behavior of the bound excitons.

In addition to the above transitions, we also observe a transition corresponding to free electron to acceptor recombination (A). This transition is very strong in α sample and becomes weaker in other quaternary alloys. In γ sample, it is observed only at high sensitivities. This is consistent with the reported observation on alloys grown by nonequilibrium (19,20) techniques where only one peak is seen for layers with compositions closer to or inside the miscibility gap region. The identity of this transition in all the quaternary layers was also further confirmed from the PL intensity dependence with the excitation intensity, which exhibit a perfectly linear variation with a slope of 1.0.

The binding energy of this acceptor can accurately be determined only if the bandgaps of the alloys are known. The bandgap in α -23 sample is obtained by adding the free exciton binding energy (~ 1.1 meV) to the free exciton transition energy (765.0 meV). The acceptor binding energy obtained in this case is about 35 meV which is in excellent agreement with the values obtained in GaSb. However, in β and γ layers, due to the absence of free exciton transition line, the band to band transition can only be estimated. If an exciton dissociation energy of 3 meV for BE_1' with a FE binding energy of 1 meV are assumed it leads to acceptor binding energies in the range of 33-37 meV which again agree quite well with that observed in GaSb.

The broad line shifted by 28-30 meV of the A peak seen towards the lower energy side in the quaternary layers has been labelled as LO phonon replica of A(A-LO), as this energy is very close to the optical phonon energy reported in GaSb (21). The ratio of the intensity of the A peak and that of A-LO peak is in the range 32-40 and remains invariant within experimental error with laser power intensity and decreases with increase in temperature. This trend is consistent with the expected behavior of the phonon sideband further strengthening the assignment of this peak.

Temperature dependence of the band to band transition was also examined in the temperature range of 4.5K to 300K. The variation of the PL peak energy corresponding to the band to band transition follows the well known empirical formulation of Varshni (22) which is given by

$$E_g = E_{g0} - [\alpha T^2 / (\beta + T)]$$

where E_{g0} represents the extrapolated value of band gap at 0°K, α and β are empirical parameters. At low temperatures, binding energy of the bound exciton was taken into

account for the estimation of the band gap transition as explained earlier. Care was taken that a good fit to data is obtained at higher temperatures ($\geq 40\text{K}$). Figure 2 shows the temperature dependence of the band gap shift for the three different alloy layers investigated. The values of α and β that resulted in a best fit to the experimental data is tabulated in Table 3. It may be noted that the value of E_{g0} is close to (within 1meV) with our earlier estimation of the bandgaps of the alloys. For GaSb the values of α and β are in excellent agreement with those reported by Camassel et al. (23). However, they are considerably larger for the other layers which may be an indication of the presence of high degree of disorder in these layers. In the temperature range of 100-300K, the linear portion of the plot exhibited a slope of $\approx -0.31 \text{ meV/K}$ for the quaternary layers. This compares well with the value of -0.37 meV/K for GaSb (23). The implication is that a variation of 7-13 Å/K could be expected in the emission peak wavelength of the lasers and LEDs fabricated from GaSb and its alloy system.

IV CONCLUSIONS

In conclusion, we have examined the near band edge PL features of LPEE grown GaInAsSb layers on (100) GaSb substrate. Considering the fact that this is a quaternary alloy system and hence even a small statistical inhomogeneity in the composition could cause sufficient potential fluctuations to result in significant spectral broadening, the values of the FWHM of the bound excitons and the presence of FE attest to the high optical quality of the quaternary layers grown. Temperature dependence of the band to band transition has also been studied.

ACKNOWLEDGMENTS

This work was supported by AFOSR (Contract No. F49620-89-C-004) and USARO (Grant No. DAAL03-89-G-0115). Work of S.H. was supported by Air Force (Contract No. F33615-88-C-5423).

TABLE I Low temperature PL features reported in LPE grown GaSb and from current study.

Ref. (1,2)		Our Work		
Identity	Energy (meV)	Energy (meV)	ΔE (meV)	Relative Intensity
FE	809.9	808.5	0.0	0.05
UI	808.7			
UI	808.0			
BE ₁	805.4	805.4	3.1	0.02
BE ₂	803.4	802.2	6.3	0.69
BE ₃	800.1	799.1	9.4	0.34
BE ₄	796.1	795.8	12.7	0.48
UI	795.0			
UI		784.8		0.09
A	777.5	777.5		1.00
BE ₄ -LO	766.0	765.6		0.03
B	757.0	756.3		0.04
A-LO	748.5	748.2		0.03
B-LO	728.0			
C	710.0			

A - band-residual acceptor transition

B - band-acceptor transition

C - second ionization level of acceptor A

ΔE - exciton dissociation energy

TABLE II Low Temperature PL features observed in LPEE grown GaInAsSb layers.

α -23				β -9			γ -11		
Iden	Energy (meV)	Rel. Int.	ΔE (meV)	Energy (meV)	Rel Int.	ΔE (meV)	Energy (meV)	Rel. Int.	ΔE (meV)
FE	765.0	0.11	0.00						
BE ₁ '				703.8	1.0	3.0 ^a	607.1	1.0	3.0 ^a
BE ₂ '	760.5	1.00	4.6	697.9	0.04	8.9 ^a			
BE ₃ '	754.3	0.48	10.7	691.1	0.07	15.7 ^a	594.1	0.02	16.0 ^a
UI	742.2	0.07							
A	730.6	0.97		670.9	0.08		578.1	0.002	
A-LO	702.2	0.03		640.2					

^a estimated value of the exciton dissociation energy (ΔE)

TABLE III. Variation of band to band transition in $\text{Ga}_{1-x}\text{In}_x\text{As}_y\text{Sb}_{1-y}$ with temperature.

$E_g = E_{g0} - \alpha T^2 / (\beta + T)$				
Sample #	λ_{PL} @ RT (μm)	E_{g0} (eV)	α ($10^{-4}\text{V}/^\circ\text{K}$)	β ($^\circ\text{K}$)
GS-8	1.70	0.810	3.80	94
α -23	1.81	0.767	6.43	329
β -9	1.96	0.706	5.28	285
γ -11	2.25	0.611	3.36	156

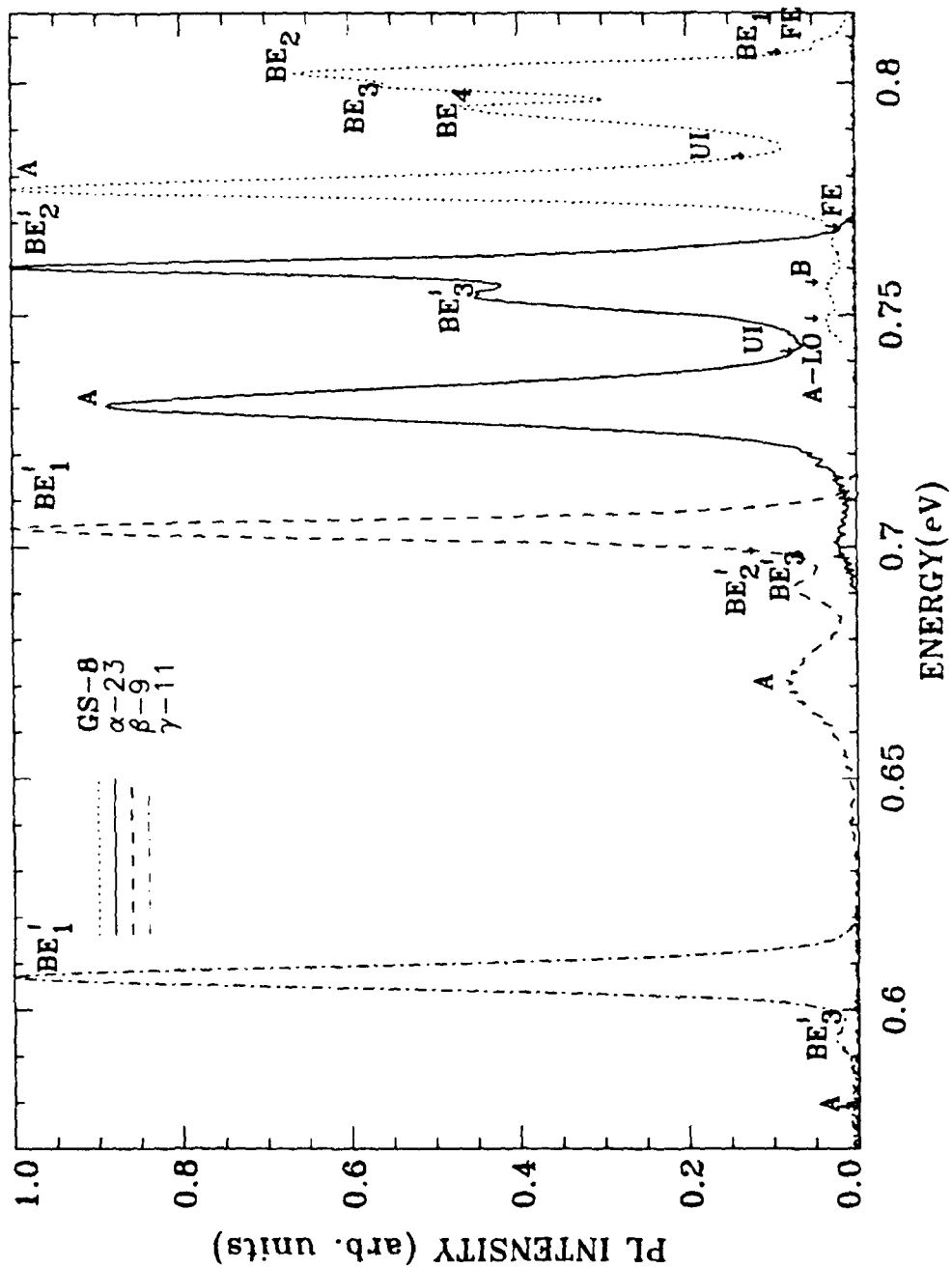
FIGURE CAPTIONS

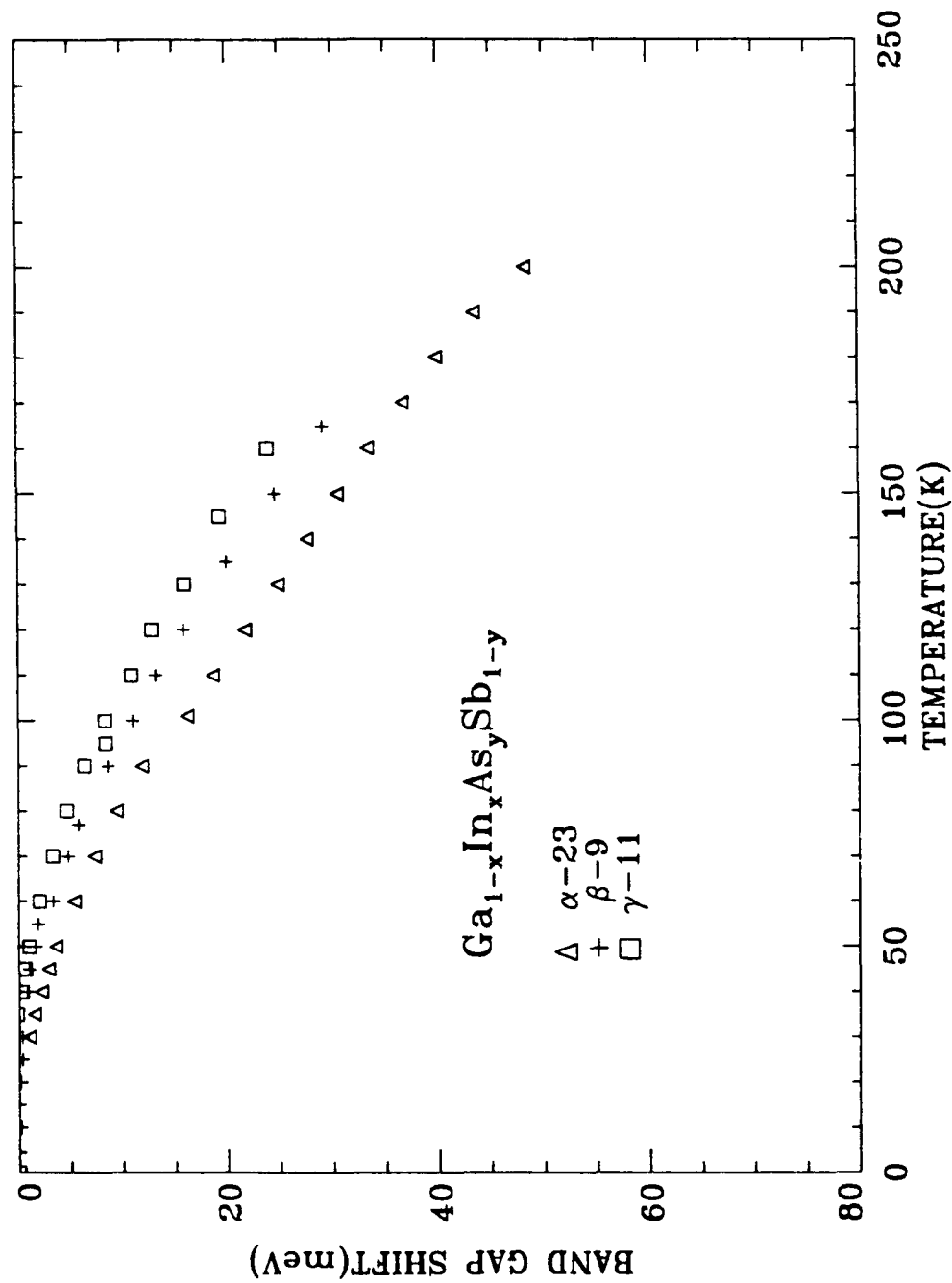
1. Low temperature (4.5K) PL spectra of GaSb and GaInAsSb of three different compositions.
2. Temperature dependence of the band gap shift for GaInAsSb layers of three different compositions.

REFERENCES

1. W. Ruhle, W. Jakowetz, C. Wolk, R. Linnebach and M. Pilkuhn, Phys. Stat. Sol.(B) **73**, 255 (1976).
2. W. Jakowetz, W. Ruhle, K. Breuninger and M. Pilkuhn, Phys. Stat. Sol.(A)**12**, 169 (1972).
3. S.C. Chen and Y.K. Su, J. Appl. Phys. **66**, 350 (1989).
4. M. Lee, D.J. Nicholas, K.E. Singer and B. Hamilton, J. Appl. Phys. **59**, 2895 (1986).
5. K.F.Longenbach and W.I. Wang, Appl. Phys. Lett. **59**, 2427(1991)
6. E.T.R. Chidley, S.K. Haywood, A.B. Henriques, N.J. Mason, R.J. Nicholas and P.J. Walker, Semicond. Sci. Technol. **6**, 45 (1991).
7. Shanthi N. Iyer, Ali Abul-Fadl, Albert T. Macrander, Jonathan H. Lewis, Ward J. Collis and James W. Sulhoff, Mat. Res. Symp. Proc. **160**, 445 (1990).
8. C.Takenaka,T.Kusunoki and K.Nakajima, J.Cryst.Growth **114** 293(1991)
9. A. Okamoto, J. Lagowski and H.C. Gatos, J. Appl. Phys. **53**, 1706 (1982).
10. J.J. Daniele and A. Lewis, J. Electron. Mater. **12**, 1015 (1983).
11. Y. Imamura, L. Jastrzebski and H.C. Gatos, J. Electrochem. Soc. **125**, 1560 (1978).
12. E.J. Johnson and H. Y. Fan, Phys. Rev. **139**, A1991 (1965).
13. C. Benoit a la Guillaume and P. Lavallard, Phys. Rev. B **5**, 4900 (1972).
14. W. Ruhle and D. Bimberg, Phys.Rev. B **12**, 2382 (1975).
15. Fred H. Pollack and R.L. Aggarwal, Phys. Rev. B **4**, 432 (1971).
16. D. Effer and P.J. Etter, J. Phys. Chem. Solids **25**, 451 (1964).

17. Y.J. Van der Meulen, J. Phys. Chem. Solids **28**,25 (1967).
18. S.Iyer, S.Hegde, Ali Abul-Fadl, K.K.Bajaj and W.Mitchel, Phys.Rev.B.(to be published).
19. S.J. Eglash and H.K. Choi, Inst. Phys. Conf. Ser. No. **120** ed.G.B. Stringfellow(American Institute of Physics,1992)p.487
20. T.H.Chiu, J.L.Zyskind and W.T.Tsang, J.Electron Mater.**16**,57(1987)
21. C.Pickering, J. Electron. Mater. **15**, 51 (1986).
22. Y.P.Varshni, Physica **34**,149(1967)
23. J. Camassel and D. Auvergene, Phys. Rev. B **12**, 3258 (1975).





S. Iyer
J. Appl. Phys.
Figure 2.

